MSc Thesis Biobased Chemistry and Technology

Effect of partial CO pressure on the acetate metabolism of *C. hydrogenoformans* and the effect of biological condition on Ru/C activity

T.M. Torres Ruano

20-9-2018

In Collaboration with the department of Microbiology

WAGENINGEN
UNIVERSITY & RESEARCH

Effect of partial CO pressure on the acetate metabolism of *C. hydrogenoformans* and the effect of biological condition on Ru/C activity

Name course	:	MSc Thesis Biobased Chemistry and Technology
Number	:	BCT-80436
Study load	:	36 ects
Date	:	20-09-2018

Student	:	T.M. Torres Ruano
Registration number	:	941110840020
Study programme	:	MBT
Report number	:	106BCT

Supervisor(s)	:	Tomas van Haasterecht and Martijn Diender
Examiners	:	Elinor Scott and Diana Machado de Sousa
Group	:	Biobased Chemistry and Technology
Address	:	Bornse Weilanden 9 6708 WG Wageningen The Netherlands

WAGENINGEN
UNIVERSITY & RESEARCH

Abstract

In recent years, biomass gasification has seen an increase in popularity as substrate for the production of biobased fuels and chemicals. Currently both biological and chemical conversion methods to obtain these product are applied. In this research a novel combined biological and chemical conversion is studied. This method has the potential to negate some of the difficulties faced by biological and chemical synthesis gas conversion. In the combined system synthesis gas is fermented to acetate and hydrogen gas by the extremophilic bacterium *Carboxydothermus hydrogenoformans*. Acetate is hydrogenated on a Ru/C catalyst to produce ethanol. This work focuses on the acetate metabolism of *C. hydrogenoformans* and the effect of biological conditions on the Ru/C catalyst. It was found that *C. hydrogenoformans* ferments CO to acetate, under elevated CO pressure of 2.7 and 4 bar, in a two-step process. First CO is converted to H_2 and CO_2 though the water gas shift metabolism, followed by the assimilation of CO_2 in the Wood-Ljungdahl (WL) pathway. An average yield of acetate on CO of 0.14±0.01 mol/mol was observed. It has been shown that WL activity is inhibited by CO, resulting in two conversion phases. A kinetic model, showing H_2, CO_2 and CO pressures as well as acetate content over time was produced. The Ru/C catalyst was shown not to hydrogenate CO in under a pressure of 16 bar H_2 and 4 bar CO. However, catalyst deactivation occurred when it was added to an active culture of *C. hydrogenoformans* for 5 days. Scanning electron microscopy images showed no sign of sterical deactivation. When the deactivating effect of individual medium components were tested, sulfide showed full deactivation. Yeast extract also showed signs of deactivation, however no significant effect was observed in the limited dataset.

Table of Contents

1. Introduction

In the past decades the rise in fuel and chemical demand, combined with the increase in greenhouse gas emissions and depletion of fossil resources, has pushed technology to find more sustainable ways to make these products. Biomass has a potential too be a replacement for some of the fossil resources used to produce fuel and chemicals today (1, 2). Fermentation of digestible sugars from designated crops is currently the most abundant production method of such bio-based products. However, to increase to production further, more biomass resources have to be utilised. Preferably waste streams, to avoid the food vs. fuel debate (3).

Gasification of biomass is in the process of becoming a viable method to turn a wide range of (waste)biomass into a potential feedstock for the bio-based industry (4). In gasification, biomass or fossil based substrates are heated to a high temperature (>700°C). A controlled amount of oxygen and/or steam is added. This results in a mixture of CO, CO_2 and H_2 called synthesis gas (syngas) (5). Several chemical (6) and biological (4) processes that utilise syngas as a substrate have been reported. Both approaches have their pros and cons. Chemical conversion, utilising the Fisher-Tropsch process, is efficient and well documented, but requires elevated temperatures and pressures. Making for high investment costs. Furthermore the catalysts susceptible to inactivation due to presence of impurities in the syngas (6). These contaminations are more abundant in syngas derived from biomass than when it is produced from fossil sources (7). This is due chemical diversity of biomass compared to fossil alternatives. Therefore, before biomass derived syngas can be used as a substrate for the Fisher-Tropsch process is has to be scrubbed. A process in which contaminants are removed. This adds to the cost and complexity of the process, making economically unviable till this day (8).

To avoid deactivation by contamination, a different type of catalyst is required. On such type catalyst are organisms, able to ferment syngas. These organisms are more resilient to contaminations in the syngas and are able to renew themselves. These fermentative processes are however limited by the gas-liquid mass transfer rate and are thus slower than the Fischer-Tropsch process (9). Furthermore, biological conversions of syngas are carried out at lower temperatures as the syngas is being produced at. The gas thus has to be cooled before it can be converted. However gas scrubbing or expensive metal catalysts are not required. Therefore fermentation could be an interesting alternative to the Fisher-Tropsch process (10). Syngas fermentation is still in an early phase of development, and more research is thus required (11). In this research a novel syngas conversion method is being investigated. In this system biological conversion is combined with metal catalytic conversion. In this setup the product(s) of the organism are converted by the catalyst. Such a system has to our knowledge not been studied yet. Syngas fermentation products are produced through the Wood-Ljungdahl pathway. This results in small carbohydrates like acetate and ethanol (10). By utilising co-cultures, medium chain fatty acids have been produced (12). All these products have a high oxygen content. Hydrogenation of these molecules would remove one or more oxygen atoms (13). This would diversify the range of products that can be derived from syngas. Hydrogenation of fermentation products would be of special interest for the production of fuels and chemicals (14). The combination of fermentation and hydrogenation in a single reactor eliminates the requirement of intermediate purification. It could decrease the capital investment of a process by reducing the amount unit of operations required.

More possible advantages of combined microbial and chemical conversion is that the microbe could consume contaminations such as NH_3 and sulfur compounds present in the syngas (15). These compounds could otherwise deactivate the catalyst. Therefore gas scrubbing may not be necessary in a combined system, decreasing investment costs. All these advantages are theoretical since there are a lot of unknowns

in such a system. Microbes have, too our knowledge, not been studied in the presence of metal catalyst. The interactions between the two is thus not known. There is the possibility that the presence of microbial material deactivates the catalyst or vise versa. Furthermore, microbes are only active in a medium suited for that organism. Some of these medium components could interact with the catalyst, either deactivating it, or resulting in an unfit medium.

Current syngas fermentations operate at temperatures between 30 and 40°C, at pressure close to atmospheric pressure (16). Chemical catalysis is currently done at temperatures exceeding 150°C and pressures over 20 bar. Due to this large difference in reaction conditions, a compromise in temperature and pressure has to be reached. Since most organism do not show any activity at temperatures more than an few degrees above their optimum, an organism normally operating at a higher temperatures is required. The extremophilic CO fermenting bacterium *Carboxydothermus hydrogenoformans* has been chosen for this reason. It has a temperature optimum of 72°C (17) and in previous work in the department of Biobased Chemistry and Technology and the department of Microbiology, is has been shown that it is active under pressures up to 20 bar (18). No higher pressure were tested. Furthermore it has been shown that this organism can accumulate acetate in the presence of CO, with indications that higher initial CO and H_2 partial pressures result in higher acetate yield (18). The relation between these two parameters has not been described yet.

Since acetate is produced by the organism, a catalyst converting acetate under mild conditions is required. For this research a Ru/C catalyst was chosen. This catalyst has been shown to hydrogenate acetic acid at 70°C and a hydrogen pressure of 58.5 bar, resulting in ethanol (19-22). Hydrogenation of acetate was not successful. This is a challenge that has to be overcome, but it is not included in this research. The purpose of the proposed system is not to be a viable industrial application. The purpose is to serve as a model system to identify problems and opportunities when combining biological conversion with metal catalytic conversion. The goal of this research is to get an insight into the combination of biological an metal catalysis.

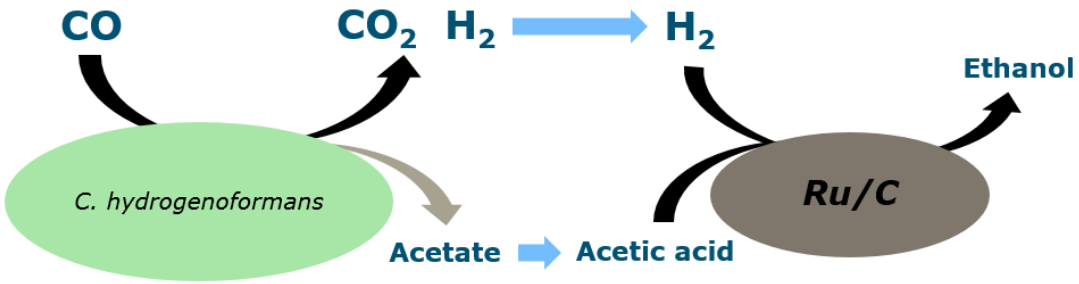

Figure 1. Schematic overview of combined biological and chemical conversion

A potential risk of using this system is that, under the conditions described above, H_2, CO and Ru/C are present at the same time. This could result in the formation of methane. No data on this reaction under the proposed conditions is available. However, methane formation would be energetically favourable.

C. hydrogenoformans

First described in 1991, *Carboxydothermus hydrogenoformans* is an extremophilic, anaerobic, chemolithoautotrophic, freshwater bacterium. The growth has been observed at a temperature range of 40-78°C and a pH varying from 6.0 to 8.0. Optimal growth conditions are at 70-72°C at a pH of 6.8-7 (17). *C. hydrogenoformans* utilises the water gas shift (WGS) pathway as its main form of energy generation. In this metabolism CO and water enter the nickel-iron CO dehydrogenase complex (CODH) resulting in CO_2 that is released. The protons and electrons, separated from the water are moved to the membrane bound hydrogenase that is physically attached to the CODH. Here the protons and electrons are combined into molecular hydrogen. The resulting energy is utilised to move proton or sodium ion over the membrane. The resulting ion gradient drives a ATP synthase (23). The combined reaction reads:

$$CO + H_2O \rightarrow H_2 + CO_2$$

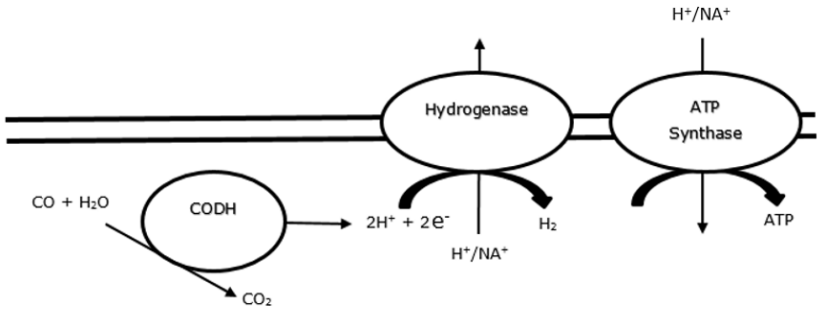

Figure 2. Schematic overview of the WGS pathway in C. hydrogenoformans.

Since *C. hydrogenoformans* is grown with CO and CO_2 as sole carbon sources, not taking into account yeast extract (YE), CO and CO_2 have to be assimilated to support growth. It has been reported that this is done though the Wood-Ljungdahl (WL) pathway (24)(Figure 3). In this pathway CO_2 is first reduced with H_2 to produce formate. The produced formate is bound to tetrahydrofolate (THF) and reduced twice with NADH as e-donor, resulting in a methyl group. The methyl group is split off the THF and is combined with a CO and CoA^-, resulting in acetyl-CoA. This than enter feeds the anabolic pathways. If no CO is available for acetyl-CoA production, it can be produced through the reduction of CO_2 with Fd^{2-} (23).

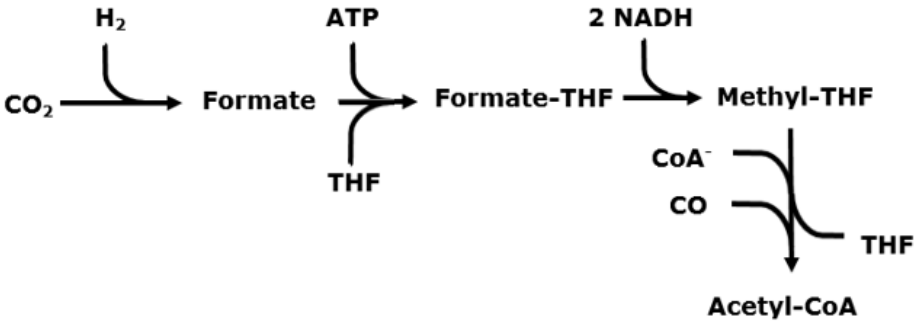

Figure 3. Schematic overview of WL pathway

Both the above mentioned pathways are common in syngas fermenting organisms (16). What is special about *C. hydrogenoformans* is that is does not shows signs CO toxicity (17). Though it is theoretically possible, *C. hydrogenoformans* has not been reported to grow in the presence of only CO_2 and H_2 (24). It should be able to convert acetyl-CoA into acetate, resulting in an ATP production. If ATP is produced through this route, the WGS pathway should no longer be required. It has been reported that *C. hydrogenoformans* contains all the genes necessary for this alternative metabolism, it has however never been observed as sole activity. Some acetate production has been reported (25) (18). This was however only observed as background activity that occurred parallel to WGS pathway activity.

Results by J. Hofman (18) show that at a high initial CO partial pressure (3-5 bar) final acetate concentrations increase considerably. Since acetate was barely produced at lower initial CO partial

pressures, the relation between CO pressure and acetate production is not fully understood. A theory from this research is that the acetate metabolism is activated due accumulation of H_2 and CO_2. This would increase ΔG of the WGS pathway, making it unfeasible. Since in this case CO would be present without the WGS pathway being active, the organism would which to energy generation through acetate production from CO, CO_2 and H_2. When *C. hydrogenoformans* would only be able to produce acetate with CO present, it would explain why acetate was only found in low amounts under normal conditions. Since the WGS pathway would in these cases be able to consume all CO without being inhibited by high product concentrations. The data shown in the abovementioned research was however not adequate for confirming this theory. Therefore, identifying the conditions under which *C. hydrogenoformans* produces acetate will be one of the goals of this research.

Ru/C catalyst

As mentioned before, ruthenium supported on activated carbon (Ru/C) was chosen as the metal catalyst for this research. Ru/C had been reported to reduce acetic acid to ethanol at a relatively low temperature of 90°C. Furthermore is was proposed that the hydrogenation mechanism would first convert the acetic acid into acetate, before hydrogenation (26). Research conducted parallel to this project pointed out that though the Ru/C was able to hydrogenate acetic acid at the biologically acceptable 70°C, hydrogenation of acetate was not possible (20).

Since the contents of the biological system are very diverse and not accurately determined, some of its components could affect the catalyst activity. Deactivation can occur in through many mechanism (27). The most likely mechanism in a combined biological system are fouling and poising. In fouling the catalyst is deactivated by the deposition of a physical material on the catalyst surface, making it unavailable for the substrate. When biomass is introduced, macromolecules such as proteins and carbohydrates are released. These could be deposited onto the catalyst. Cells could also produce a biofilm on the catalyst surface, resulting in deactivation.

Deactivation through poising occurs by strong chemisorption of a molecule on the catalyst surface. The presence of the molecule can physically block the catalyst or disturb the electrons on the catalyst surface around it, resulting in an increased deactivated area (28). Sulfur compounds are notorious for their poisoning effect on metal catalyst. Therefore growing *C. hydrogenoformans* without the addition of sulfur compounds such as sulfide will be looked into in the research.

Goals

The goal of this research is to get a better understanding of the individual components of the proposed combined biological and chemical conversion. For this goal the following research question has been setup:

What is the effect of partial CO pressure on the acetate metabolism of *C. hydrogenoformans* and how do its biological conditions affect the activity of Ru/C catalysed hydrogenation of acetic acid?

To answer this question the following research areas will be studied.

- The effect of partial CO pressure on the acetate metabolism of *C. hydrogenoformans*.
- Effect of Ru/C the viability and activity of *C. hydrogenoformans.*
- Deactivation of Ru/C catalysed acetic acid hydrogenation by compounds found in biological medium.
- Hydrogenation of CO in presence of Ru/C and H_2.

2. Materials and methods

Chemicals

All chemicals were purchased from Sigma Aldrich (Germany) with exception of ethanol which was purchased from Merck (Germany)

Organism

Carboxylothemus hydrogenoformans Z-2901 (DSM-6008) was ordered from the German Culture Collection (DSMZ, Germany).

Medium

In this reaches a standard growth medium used in the department of Microbiology, developed by was used. This medium was produced in two stages. First a mineral solution was prepared and autoclaved at 121°C for 20 minutes. This solution contained 0.41g/L KH_2PO_4, 0.36g/L $Na_2HPO_4.4H_2O$, 0.3g/L NH_4CL 0.3g/L NaCL, 0.1g/L $MgCl_2.6H_2O$ 61.8µg/L H_2BO_3, 61.25 µg/L $MnCl_2$, 943.5µg/L $FeCl_2$, 64.5 µg/L $CoCl_2$, 12.86µg/L $NiCl_2$, 67.7µg/L $ZnCl_2$, 13.35µg/L $CuCl_2$, 17.3µg/L Na_2SeO_3, 29.4µg/L Na_2Wo_4 and 20.5µg/L Na_2MoO_4. To this solution 0.5 mg/L resazurin was added as a marker for oxidising agents such as oxygen. To remove oxygen, the solution was boiled for no more than 30 seconds. After boiling it was cooled on ice and pumped into glass flasks under continuous N_2 flow. To the flasks rubber stoppers and aluminium caps were added. The headspace of the filled flasks was filled with N_2/CO_2 (4:1) to an absolute total pressure of 1.5 bar. At this point flasks were stored up to two months.
Before inoculation, 5%v reducing and buffering agent was added, containing 80g/L $NaHCO_3$ and 4.7g/L Na_2S. 2%v 50g/L yeast extract solution and 2%v calcium/vitamin solution containing 10g/L $CaCl_2$ and vitamins was added

Experiment setup

Shake flask

To do low pressure experiments, up to a maximum of 3 bars absolute total pressure, 117 or 250 mL shake flasks were used. Flasks were filled with either 34.5 or 51.5 mL medium and capped with a rubber stopper. Final medium components were added after autoclavation, (121°C 20min) shortly before inoculation. An inoculum volume of 1.0 mL active culture was used. CO was added by first removing the N_2:CO_2 (4:1) gas in the headspace to approximately atmospheric pressure and manually adding pure CO, using a 50 mL syringe. During the experiments gas and liquid samples could be taken using a 1.0 mL syringe. Experiments were designed such that no more than 10% liquid or gas volume was sampled in total.

High pressure Parr system

To test the effect of high CO partial pressure on the metabolism of *C. hydrogenoformans* a set of high pressure experiments was set up. Experiments were carried out in parr 5000 multi reactor system (Parr Instruments Company, USA). Glass sleeve were added to the reactors to avoid contact between the liquid in which conversion took place. Total volume of the individual reactors available for gas/liquid equals 68.9±0.9 mL. For each experiment liquid was added composing of either 15 mL fresh medium and 15 mL culture or 35.5 mL fresh medium with 0.5 mL culture. These inoculation ratios will be referred to as large and small inoculum respectively. 6 mL fresh medium was added between the reactor wall and glass sleeve for heat transfer from the walls to the sleeve. The reactors were filled in an anaerobic tent with a headspace composition of N_2:H_2 (50:1). Due to limitation in the setup, sterile inoculation was not possible. After removing the reactors from the anaerobic tent, the headspace was flushed 4 times with N_2:CO_2 (4:1). After the 4^{th} flush, pressure was allowed equilibrate with atmospheric pressure. Flushing the headspace is required since some CO_2 needs to be present in the headspace to utilise the carbonate buffer present in the medium. At this point the reactors were moved from the laboratory of microbiology to the laboratory of biobased chemistry and technology.

Here, CO or CO_2 was added though the gas outlet valve of the reactor until the desired pressure was reached. After filling the gas outlet was capped to prevent leakage though the gas outlet valve. Due to limitations in the setup, CO and CO_2 pressure could not exceed 4 and 3 bar respectively. Once the CO or

CO_2 was added, the reactors are moved to the parr 5000 multi reactor heating system and connected. The gas filling lines of the Parr system were connected to the reactors to prevent CO from leaking into the room. If H_2 was required it was added through this gas inlet line, by first flushing the manifold 6 times with N_2 and 6 times with H_2. Note that the section between the before mentioned gas inlet valve of the reactors and check valve in the inlet line is not flushed in this process. To flush this section the manifold must first be pressurised and depressurised with N_2. The section between the check valve and inlet valve of the reactor is now pressurised. Release the pressure from this section by opening the valve located on the connection between gas filling line of the parr system and the gas inlet of the reactor. Repeat this procedure 6 times. Flushing this section with H_2 is not possible because H_2 would be released into the room.
In one of the experiments, CO has to be introduced to the headspace during operation. To do this a secondary headspace that is connected to the main headspace is required. This secondary headspace consists of a 20 cm piece of tubing, with an inner diameter of 3mm, closed at both ends with needle valves. One of the valves connect to a unutilised port in the Parr reactors. The total volume of this secondary headspace was determined to be 2.75±0.03 mL. It is assumed that CO present in the secondary headspace finds its way to the main headspace though diffusion.
The controller was set to heat the reactors from room temperature to 70°C in 4 hours. After this the temperature was kept constant at 70°C. This profile was programmed individually for each reactor. Temperature and total pressure measurements were logged every 10 seconds. Temperature readings we only used to check proper operation. To reduce the amount of data produced by the logging, the average of the pressure measurements over a period of 10 minutes was used for further calculations and graphical representation.

Analytical techniques

Liquid composition

HPLC

To measure biological and catalytic activity, two different HPLC setups were used in this research. Samples from microbiological experiments were measured at the department of Microbiology with a TSD-HPLC (thermo Scientific, Waltham, USA) on a MetaCarb 67H column (Agilents Technologies, Santa Clara, Canada). The eluent was 0.01M H_2SO_4 at a column temperature of 45°C. Both a IR- and UV-detector were used. To remove solids from the samples, they were centrifuged at 13000 G for 4 minutes. Due to variation in loading volumes 2:3 (sample:internal standard)10mM DMSO was added as internal standard. 5 mM DMSO was chosen. Acetate, Formate and Ethanol were calibrated from 0.125 to 10 mM.
Samples from catalyst experiments were measured using a Dionex Ultimate 3000 RS auto sampler HPLC on a BioRAD 125_0146 column at 50°C. 5mM H_2SO_4 was used as eluent. Detection was done by UV and IR. No internal standard was applied. Acetic acid was calibrated from 5 ot 100 g/L. Ethanol was calibrated from 0.1 to 5 g/L.

Gas composition

Shake flasks

For each gas measurement 0.28 mL gas, at flask pressure, was sampled and diluted to 1.08 mL in a 1.0 mL syringe. 0.08 mL gas is present in the tip of the syringe, which the scale does not account for. 1.0 mL sample was injected into a Compact GC 4.0 (Global Analyser Solutions). CO, CH_4 and H_2 were separated using a molsieve 5A column at 100°C. CO_2 was separated on a parallel column (Rt-T-BOND) at 80°C. All gasses were deleted on a thermal conductivity detector. `
To find the volume of either CO_2, H_2 or CO in the headspace of the flask equation 1 was used

$$V_x = \frac{a_x}{a_x^{cal}} * p_x^{cal} * V_{headspace} \qquad \textit{Equation 1}$$

V_x Volume of either CO_2, H_2 or CO at atmospheric pressure (mL). a_x peak area of gas (mV*min). a_x^{cal} peak area of a calibration standard of the same gas (mV*min), p_x^{cal} partial pressure of the gas in the calibration standard. $V_{headspace}$ volume of the flask headspace (mL).

Parr system

Gas samples from the high pressure setup were only taken at the end of each batch. The reactor are cooled by setting the temperature set point to 20°C and removing the reactors from the heating elements. Once cooled to 20-30°C, the gas outlet valve was opened for short intervals until the pressure dropped under 2.5 bars. At this point a piece of plastic tubing (4 cm, inner diameter 4 mm), onto which a syringe could be mounted, was fitted to the gas outlet. The first gas sample (±10 mL) was discarded to flush the setup. The second sample (15-25 mL) was injected into an air tight, 50 mL flasks. From this flasks three normal gas samples were measured as described above. The ratio of H_2, CO and CO_2 was calculated. From these ratio's the gas composition in the reactor was calculated using equations 2 and 3**.** In this calculation it is assumed that N_2 is not consumed or produced. that all other gasses present are either CO_2, H_2 or CO and that there are conversion after the reactors start cooling.

$$fraction_{CO} = \frac{\frac{a_{CO}}{a_{CO}^{cal}} * p_{co}^{cal}}{\frac{a_{CO}}{a_{CO}^{cal}} * p_{co}^{cal} + \frac{a_{CO_2}}{a_{CO_2}^{cal}} * p_{co_2}^{cal} + \frac{a_{H_2}}{a_{H_2}^{cal}} * p_{H_2}^{cal}} \qquad \textit{Equation 2}$$

$$p_{co} = (p_{tot}^{reactor} + 1 - p_{N_2}) * fraction_{CO} \qquad \textit{Equation 3}$$

$fraction_{CO}$ the ratio of CO volume to the combined CO, CO_2 and H_2 volume (-). $p_{tot}^{reactor}$ total pressure in the reactor at the point which cooling starts (bar) .p_{N2} nitrogen pressure (bar).

It is assumed that nitrogen is not produced or consumed during all conversions. Note that the +1 is there to correct for the fact that the reactor pressure is assumed to be 0 bar at atmospheric pressure.

Solid composition

Dry weight

Dry weight content could not be accurately determined. At the high temperature, precipitated was produced that did not re-dissolve into water after centrifugation of all solids. Blanc, sterile flasks showed varying dry weight contents.

Scanning electron microscopy

Catalyst samples were freeze dried and gold plated. SEM images were produced with a FEI Magellan 400 SEM with Aztec EDS system. A TLD detector was used. Voltage and magnitude setting are displayed within the SEM images.

Data processing

Calculation

Model calculation were done in MATLAB R2016b. All other calculations were processed in Microsoft Excel 2016.

Statistical analysis

Experimental results were tested in a two sample unequal variances t-test. A p value of 0.05 was applied.

3 Results and discussion

3.1 Effect of CO partial pressure of acetate production

In previous work acetate production by *C. hydrogenoformans* has been observed (18). The source of this production has not yet been identified. CO was used as substrate, however before the effect of CO pressure can be studies, the effect of medium component and CO2 on the acetate production have to be looked into. Once these effects have been established, the effect of CO pressure on acetate production can be investigated.

3.1.1 Acetate production from yeast extract

With CO as a substrate, acetate production has been observed in previous experiments (18). The source of this acetate, which could be either the CO substrate or yeast extract was not identified. In order to investigate if the effect of medium the acetate production, experiments with a minimised amount of CO substrate and a varying amount of yeast extract(YE) were performed. To investigate the production of acetate from yeast extract, shake flasks are inoculated with varying concentrations of YE. Under normal conditions 1 g/L YE is used, in this experiment a range of 0 to 4 g/L YE is tested. 35mL CO is added to all flask. Acetate concentration is measured after 2 days.

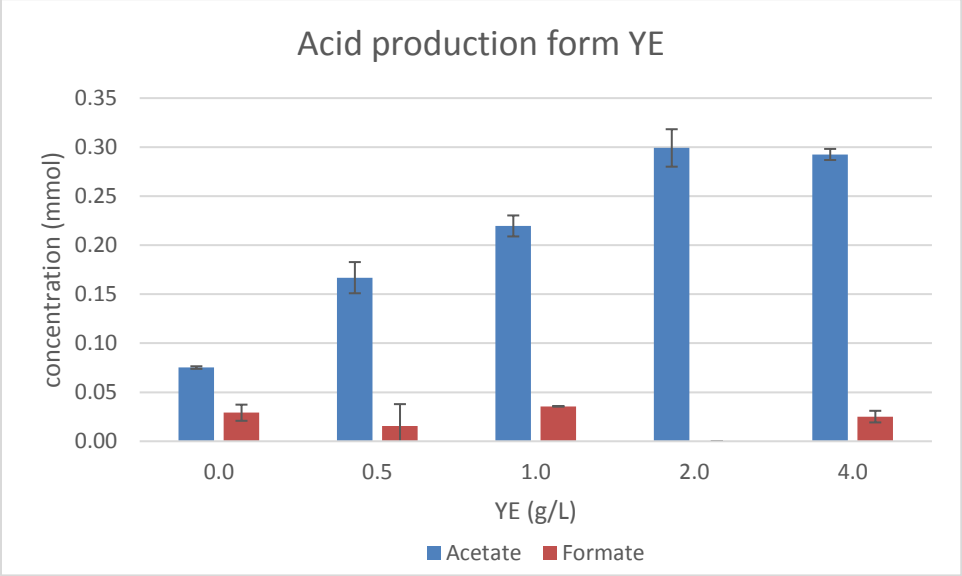

Figure 4. final acetate and formate content with varying YE concentrations produced by C. hydrogenoformans from 35 mL (1.56mmol) CO. Measured in duplicate, standard deviation given by error bars.

As can be seen in Figure 4 , the initial YE concentration has an impact on the amount on acetate produced. No significant difference (p=0.71) in acetate concentration was observed between samples with 2.0 and 4.0 g/L YE added. This can be due to the YE to acetate metabolism being linked to growth. This would result in an equal amount of acetate produced, when the amount of CO added is not sufficient to result in enough growth to co-convert all YE to acetate.

Some formate was found in the background, the concentration of which is not affected by YE concentration. Formate is an intermediate in the synthesis of acetate from CO in the WL pathway (29). Its presence in concentrations several factors lower than the acetate concentration is thus to be expected.

From this experiment it can be concluded that *C. hydrogenoformans* produces acetate from both CO and YE, since even with 0.0 g/L YE still a significant amount of acetate was produced. To find the yield of acetate on CO, the 0.0 g/L YE flask was refilled with CO after CO concentration was no longer detected. This was done a total of 4 times, resulting in 7.8 mmol of CO being converted to 0.40±0.06 mmol acetate. This resulted in an acetate on CO yield of 0.051±0.01 mol/mol.

To find the acetate concentration due the consumption YE under normal condition, the acetate produced with 0.0 g/L YE was subtracted from the acetate concentration found using 1.0 g/L. A acetate concentration of 2.78±0.21 mM was found. Since this value is not dependent of liquid of gas volume, it is subtracted from all further acetate concentrations.

3.1.2 Effect of CO_2 partial pressure on acetate production

In the previous experiment it has been established that acetate is produced from CO. Since for the production of acetate through the WL pathway, CO_2 can be consumed, its presence could affect the final acetate content. Therefore the possible effect of changing CO_2 pressure was investigated. To test the effect of CO_2 partial pressure on acetate production, cultures where grown in shake flasks under a headspace of CO_2 and CO. CO_2 partial pressure ranged from 0.60 to 0.95 bar. CO was added until a pressure of 1 atm. Results are compared to a blanc series with filled with 0.10 bar CO_2, 0.50 to 0.85 bar N_2, filled with CO to 1 atm. Because the medium is carbonate buffered, CO_2 could not be left out completely in the blanc series.

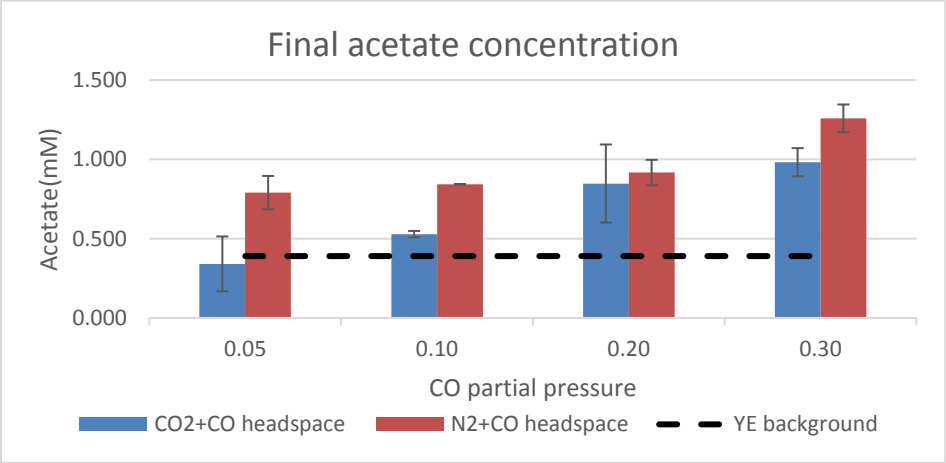

Figure 5. Final acetate concentration found after 27h of cultivation under CO2+CO (blue) or N2/CO2 (4:1)+CO (red) headspace. Dashed line represents expected acetate production due to conversion of YE. All initial total pressures are set to 1 atm at room temperature. Measured in duplicate, standard deviation is shown by the error bars. In all samples more than 95% of initial CO was consumed.

The results in Figure 5 show the final acetate content for samples containing either a CO_2 rich or N_2 rich headspace. Acetate concentration at in initial CO pressure of 0.05 or 0.10 bar were close to the detection limit, resulting in large standard deviation. When comparing the amount of acetate produced with equal initial CO pressure is stands out that samples with a CO_2 rich headspace showed a lower final acetate content. However, due to the inaccuracy of the measurements it cannot be concluded that a CO_2 rich headspace results in a lower final acetate content.

3.2 high pressure CO fermentation

Now the effect of YE and CO_2 pressure have been described, the effect of CO pressure on the acetate production by *C. hydrogenoformans* can be studied. To do this the organism had to be cultivated at elevated pressure. Therefor a autoclave reactor (Parr system) was used. In previous gas fermentations done in the Parr system, results were inconsistent. During this research is was established that flushing the reactor headspace with N_2/CO_2 (4:1) to atmospheric pressure and heating the reactors over a period of 4 hours helped gain more consistent results.
To test the effect of p_{CO} on the acetate production of *C. hydrogenoformans*, initial p_{CO} of 1.2, 2.7 and 4 bar were tested. Total pressure was measured over time. At the end of incubation, gas and liquid composition was determined. In this chapter results and observations of these experiments are discussed.

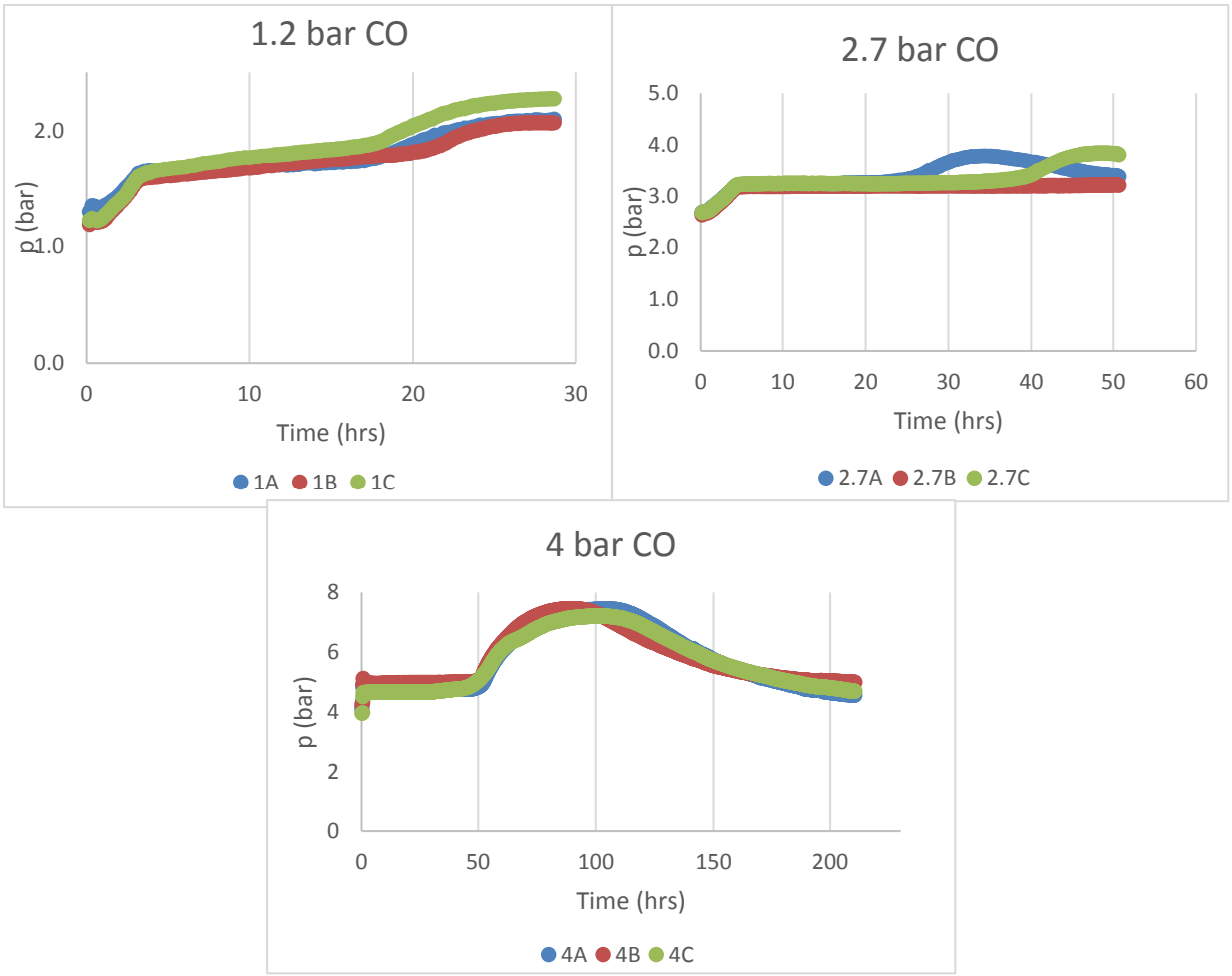

Figure 6. Pressure curves Pressure curves output of the Parr system with C. hydrogenoformans under 1 atm N_2/CO_2 (4:1) and CO pressure of 1.2 bar (1.72mmol) top left, 2.7 bar (3.79 mmol) top right and 4 bar (5.87 mmol) on the bottom.

Table 1. Contents of headspace and liquid phase before and after fermentation in mmol. Carbon balance is corrected for dissolved CO2 and formate (data not shown).

	$CO^{t=0}$ (mmol)	$CO_2^{t=0}$ (mmol)	H_2 (mmol)	CO (mmol)	CO_2 (mmol)	ACE (mmol)	$Y_{ACE/CO}$ (mol/mol)	C balance (%)	e^- balance (%)
1.2A	1.72	0.29	1.08	0.68	1.09	0.02	0.01	62	106
1.2B	1.72	0.29	1.15	0.43	1.23	0.07	0.04	63	105
1.2C	1.72	0.29	1.33	0.26	1.48	0.06	0.04	67	105
2.7A	3.79	0.29	1.47	0.54	2.42	0.41	0.12	109	90
2.7B	3.79	0.29	0.07	3.68	0.46	0.00	-	77	99
2.7C	3.79	0.29	1.60	1.59	1.79	0.13	0.06	104	96
4A	5.87	0.29	2.12	0.01	3.78	0.89	0.15	91	89
4B	5.87	0.29	2.33	0.00	4.12	0.87	0.15	96	91
4C	5.87	0.29	2.34	0.00	3.74	0.85	0.14	89	90

3.2.1 Initial CO partial pressure of 1.2 bar.

15ml of active *C. Hydrogenoformans* culture was filled to 30 mL with fresh CP-medium and flushed with N_2/CO_2 (4:1). A p_{CO} of 1.2 bar was applied and incubated at 70°C for 28h. Figure 6 and Table 1 show the obtained pressure curve and composition of gas and liquid phase.

In Figure 6, initially a rapid increase in pressure is observed during the first 4h of incubation. This is due to the heating of the reactor. After this, it can be clearly observed that the pressure keeps increasing, after a stable temperature is reached. There must thus be production of gas. This indicates the activity of the water gas shift (WGS) pathway, in which CO in converted into CO_2 and H_2, yielding a net gas production. During the first 12-17h after the heating phase, the increase in pressure is slow and nearly linear. Indicating that the activity of the WGS pathway is constant. Failed experiments, in which no activity was observed, pressure remained stable after the initial heating phase. This indicates that the pressure increase is due to biological activity. This linear phase is assumed to be the lag phase. After the lag phase, WGS activity increases. Quickly after the increase in activity, it slows down again and the reactors are stopped after 29h (cooling phase not show).

Comparing the curves at an initial p_{CO} of 1.2 bar in Figure 6 with the corresponding final CO content given in Table 1, it can be seen that even though in the end almost no pressure increase is observed. This indicates activity has stopped. However, 15-40% of the initial CO is still present. Yields of acetate on CO ranged from 0.01 to 0.04 mol/mol. This is lower than found in shake flask cultures. Results from reactor 1A suggest that when smaller a smaller amount of CO is consumed, the yield of acetate on CO is also lower. This can be due to a larger fraction of CO being consumed in the lag phase. Here the metabolism can be different, resulting is less acetate per mol of CO.

In this set of experiments the carbon balances did not close for more than 68%. The total amount of carbon in the system cannot accurately be calculated because to the pH of the system during the experiment is unknown. This makes it impossible to find the concentration of dissolved CO_2. To estimate the dissolved CO_2 concentration a pH of 7 is assumed, there is however no way to verify this assumption in the parr setup, resulting in an inaccurate carbon balance. To avoid the unknown concentration of dissolved CO_2, an electron balance was produced. In this balance CO_2 does not have to be taken into account. Since the electron balance closes around 105%, it can be assumed no non-identified products are produced during fermentation.

3.2.2 Initial CO partial pressure of 2.7 bar.

To achieve higher a higher final acetate content and to study the effect of increasing the p_{CO} on the metabolism of *C. hydrogenoformans,* a p_{CO} of 2.7 bar was applied. Other than a variation in p_{CO} the same setup as described above was used. However, due to longer lag phase, a longer incubation time was required. Under these conditions *C. hydrogenoformans* showed a different pressure curve compared to the curve obtain with a p_{CO} of 1.2 bar CO (Figure 6).

After a lag phase of 19 and 29h, total pressure increased. A peak pressure of 3.8 bar was reached after 34 and 48h. After this peak the pressure decreased, indicating consumption of gas (Figure 6). To test if the same pressure pattern would have occurred in experiments 1.2A-C, if they were continued further, the experiment was repeated over a longer time (120h). No decrease in pressure was observed (appendix Figure 17).

Comparing the amount of acetate produced in reactors 2.7A and 2.7C, it becomes clear that during the gas consumption phase, acetate is being produced. The only substrates available for this production are H_2, CO_2 and CO. Therefore the acetate must be produced through activity of the WL pathway. It was already known that the key enzymes of WL pathway is present in the genome of *C. hydrogenoformans* (24). Its activity, other than during biomass formation, was however not observed before. A possible explanation for this is that the WL pathway in this organism appears only to be active at higher H_2 partial pressures. These higher pressures have not been tested before. This is observed during the last hours of the experiment 2.7A. The H_2 partial pressure at this point is around 1.2 bar, yet the rate of the WL pathway appeared very low. Suggesting that is will not be able to consume all the H_2 as is reaches a minimum required H_2 partial pressure.

reactor 2.7B did not show any activity besides conversion of YE to acetic acid.

3.2.3 Initial CO partial pressure of 4 bar.

C. hydrogenoformans was exposed to a p_{CO} of 4 bar in the same setup as described above. Incubation time had to again be increased, due to increase in lag phase duration and a longer fermentation activity. An initial p_{CO} of 4.0 bar resulted in a similar pressure curve as seen in experiment 2.7A. Note that lag phase duration for this set of experiments was roughly twice as long. This increased lag phase duration can be caused by the temperature overshoot, that occurred due to an error in the temperature ramp programme of the Parr system. Maximum growth temperature for *C. hydrogenoformans* is found to be 78°C (17). All three reactors reached temperatures of 85-90°C. This could have killed the majority of the cells, resulting in a longer duration before growth could be observed, due to the exponential nature of growth that follows lag phase. A second option is that higher p_{CO} results in a longer lag phase, due to its toxicity (29).

3.2.4 Pathway activities during high pressure CO fermentation

CO fermentation at and initial p_{CO} of 2.7 and 4 bar showed a clear similarity in pressure curve. The pressure peak indicates a two-phase process. It is however not yet known why these pressure curves show a clear peak pressure. Results show the production of H_2, CO_2 and acetate, indicating the activity of both WGS and WL pathway. However, if the WGS and WL pathways were to be equally active at the same time, the H_2 and CO_2, produced by the WGS pathway, should be directly consumed by the WL pathway. Since the WGS produced H_2:CO_2 in a 1:1 ratio and the WL pathway consumes H_2:CO_2 2:1, some CO_2 should be left over, resulting in a gradual increase in pressure over time. If the WL pathway would not be active during the pressure increase phase, pressure would accumulate due to H_2 and CO_2 production by the WGS pathway. In a separate experiment the yield of H_2 and CO_2 on CO in the WGS pathway were investigated (appendix Table 7). In this experiment it was found that the pressure would accumulate until 1.65 times the initial p_{CO}, plus the initial N_2/CO_2 pressure, if the WL pathway would not be active. When a peak pressure value smaller than this is found, some to the H_2 and CO_2 must have been consumed by the WL pathway. In experiments 4A-C a 1.5 to 1.6 fold pressure increase was observed. Indicating some limited activity of the WL pathway during pressure increase.

When the pressure curve and final H_2 content of 2.7A is compared those in 4A-C (Figure 6 and Table 1), it is again observed that the WL pathway stops, while H_2 is still present. Final p_{H2} in 4A, 4B and 4C were measured at 1.7, 1.9 and 1.9 bar respectively. This is considerably higher than the p_{H2} of 1.3 bar, that was found at the end of experiment 2.7A. A possible explanation for this high final p_{H2} could be that the reduction potential of H_2 is no longer sufficient for the reduction of ferredoxin when final p_{H2} is reached. The required reduction potential for the reduction of ferredoxin is close to that of H_2 under standard conditions (1 bar H_2, pH 7) (30). When H_2 is reduced, protons are produced, thus at a lower pH the reduction potential decreases. If this theory is correct, the final pH in experiments 4A-C has to be lower, thus requiring a higher p_{H2} to be able to reduce ferredoxin. In experiments 4A-C, more acetate has been produced. When acetate is produced, a proton produced with it (22), lowering the pH. Furthermore, in experiment 2.7A a final p_{CO2} of 2.0 bar was found compared to an average p_{CO2} of 3.13±0.17 bar in experiments 4A-C. the increased p_{CO2} in 4A-C also indicates a lower final pH in this experiment. This theory however only holds if no bifucation enzymes are present in *C. hydrogenoformans*. Since these enzyme can lower the required p_{H2} for ferredoxin reduction by utilising other electron donors such as NAD(P)H (30).

3.3.1 Acetate production during gas accumulating phase

In the high pressure CO fermentation experiments two stage fermentation was observed. To determine when acetate is produced, the activity of the WL pathway during the gas accumulation phase has to be measured. For this, gas and liquid samples at peak pressure are required. Therefore the experiment at an initial p_{CO} of 4 bar was repeated and stopped at peak pressure. To simulate the effect of the temperature overshoot in experiment 4A-C an inoculum volume of 1.0 mL was used instead of the previously used 15 mL. Fresh medium was added to a volume of 30mL in all experiments. Results can be found in Figure 7 and Table 2. It should be mentioned that 4D did not reach peak pressure yet, due to limited laboratory opening hours.

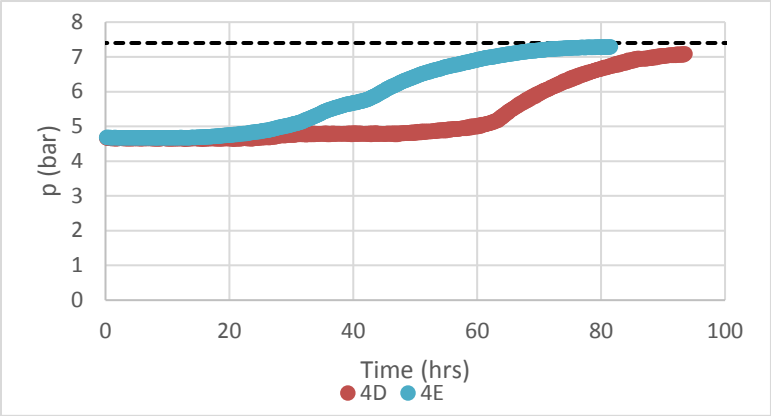

Figure 7. Pressure curves output of the Parr system with C. hydrogenoformans under 1 atm N2/CO2 (4:1) and 4.0 bar (5.87 mmol) CO. Low biomass concentration at inoculation was used. Dashed line represents the peak pressure in experiments

Table 2. Contents of headspace and liquid phase before and after fermentation in mmol. Carbon balance is corrected for dissolved CO2 and formate (data not shown).

	$CO^{t=0}$ (mmol)	$CO_2^{t=0}$ (mmol)	H_2 (mmol)	CO (mmol)	CO_2 (mmol)	ACE (mmol)	$Y_{ACE/CO}$ (mol/mol)	C balance (%)	e^- balance (%)
4D	5.87	0.29	5.09	0.42	3.53	-0.03	0.01	98.1	92
4E	5.87	0.29	5.27	0.08	3.87	-0.02	0.01	96.5	90

Figure 7 shows that final pressure in experiments 4D and 4E closely resemble the peak pressure obtained in 4A-C. Measured final acetate concentration were not significantly different from the background concentration due to YE ($p>0.6$ for both 4D and 4E). Correcting for the background concentration resulted in negative concentrations (Table 2). Judging from these final acetate contents, it can be concluded that average activity of the WL pathway activity was absent or neglectable, during the pressure increasing phase. Comparing final acetate contents of experiments 4A-C and 4D-E shows that acetate was only produced during the gas consumption phase. In experiments 2.7A and 2.7C the same conclusion was drawn, however in the set of experiments at 4 bar it is observed more clearly. Data in Table 2 also gives insight into why the WL pathway did not activate sooner, before peak pressure was reached. Here it can be seen that more than 90% of initial CO has been consumed, before the WL pathway becomes active. CO is a known inhibitor of the WL pathway (31, 32). Thus when CO is still present the WL pathway inhibited. The activity of *C. hydrogenoformans* in this batch operation can therefore be divided into 3 phases: lag phase, a WGS phase, in which WL activity is inhibited and WL phase in which no CO is present.

A second conclusion from this data is that the acetate is only produced from H_2 and CO_2, not CO. Since, at peak pressure, not enough CO is left to produce acetate in the amounts found in 4A-C from. The yield of acetate on H_2 was found to be 0.28 mol/mol, assuming all CO still present would first be converted to H_2. This is higher the maximum theoretical yield of acetate on H_2. It is assumed that this overestimation is due to the fact is was calculated from two different experiments and the error introduced by the gas sampling procedure.

3.3.2 CO spike

An experiments to verify the CO inhibition on the WL pathway was setup. In this experiment the initial headspace would consist out of 1 atm N_2/CO_2 (4:1), 3 bar CO_2 and 4 bar of H_2. These values were chosen to represent the gas composition of the pressure peak in previous experiments. Three of the Parr system reactors were modified such that a 2.75±0.03 mL piece of tubing was connected to the headspace of the through a needle valve. This piece of tubing was filled with 5 bar CO, absolute pressure. In theory, *C. hydrogenoformans* could activate the WL pathway under the conditions applied. A decrease in pressure after a lag phase would indicate this activity. At this point, the needle valve would be opened. This would

introduce small amount of CO into the system through diffusion. The effect of CO inhibition could be studied this way. when no activity were to be observed after 3 days, the valve would also be opened. If WL activity would start within 2 days after introducing CO, it would indicate CO is required for activity of *C. hydrogenoformans*. Three unmodified blanc reactors, with similar initial gas composition were tested in parallel. To these reactors no CO would be added.
after 5 days of incubation no activity of both pathways was observed. Two of the reactors showed pink resazurin, indication oxygen contamination. A possible explanation for the lack of activity could be oxygen contamination of the CO_2 stock. The H_2 stock was used in other experiments that were successful, thus this is not suspect. A second theory is that due to the high p_{CO2} the cells died in a pH shock. In experiments 4A-E an equal p_{CO2} was reached. This was however accumulated over a minimum of 35h. In the CO spike experiment the reactors were filled rapidly with CO_2.
To test if pH shock was the cause of the lack in activity, a follow up experiment was done in shake flask. To these flasks a p_{CO} of 0.03 to 0.65 bar was applied along with a p_{H2} of up to 2.8 bar and p_{CO2} of 0.2 bar. Only small amounts of acetate, in line with the yield of acetate on CO in experiments 1.2A-C, were measured after 5 days of incubation (appendix page 30). Under these conditions *C. hydrogenoformans* did thus not show sole WL activity, as observed in 4A-C and 2.7A.

3.3.3 Acetate production from CO with high biomass concentration

A third set of experiments in the parr system was executed in order to study the effect of high biomass concentration on acetate production. An initial p_{CO} of 4 bar was applied. In this set of experiments an initial biomass concentration equal to those of experiments 1.1A-C and 2.7A-C was used.

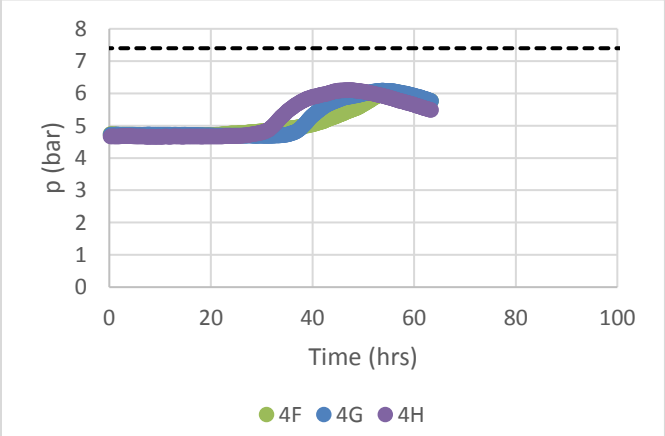

Figure 8. Pressure curves output of the Parr system with C. hydrogenoformans under 1 atm N2/CO2 (4:1) and 4.0 bar (5.87 mmol) CO. Dashed line represents the peak pressure in experiments 4A-C.

In 4F-H a lower peak pressure was observed compared to 4A-E (Figure 8). This means that with a higher initial active biomass concentration, the WL pathway becomes active sooner after the lag phase ends. This also means that it becomes active at a higher p_{CO}, since less CO has been consumed at this point. Increasing the biomass concentration would result in a lower CO concentration in the liquid phase (CO_L) (appendix page 31). If CO inhibits the WL pathway, a lower CO_L would result in a higher WL activity. By this theory the WL pathway could activate at a higher p_{CO}. Gas consumption by the WL pathway would thus start sooner when a higher biomass concentration is applied. This is in line with the observation in Figure 8. A mathematical derivation of this theory can be found in appendix page 31.

4 Modelling acetate production kinetics

In the above mentioned experiments it is already indicated that the WL pathway must be active during the fermentation. The rate of this activity is however not directly deducible from the experiments. A relation between p_{H2}, p_{CO} and the biomass concentration is implied. However, from the data shown above it cannot accurately be determined how the variables affect the pathway activities. A model describing the actual rates of the WGS and WL pathway would be a useful tool in finding these relations. From the conducted

experiments, enough data was collected to describe the p_{CO}, p_{H2}, p_{CO2} and acetate content over time though a kinetic model. This can be done by fitting the rate of the WGS pathway, combined with the yields in the observed WGS, to the pressure curve shortly after the lag phase stats. From this data, a simulation of the a pure WGS activity can be produced. The deviation between the pressure simulated and the observed pressure must be due to gas consumption by the WL pathway. A detailed description of this model and its assumption follows below.

Looking at the pressure curves of experiments 4A-F, it can be seen that after the lag phase, the activity of the WGS activity increases exponentially. This exponential increase is however not maintained for more than several hours. This can be seen in the curve since the slope first quickly increases over time and after reaching a maximum, slowly decreases again. At this maximum rate, the rate at which CO dissolves can no longer keep up with the increasing demand of CO by the organism. Limitation switches from limitation by biomass concentration, to limitation by gas transfer rate. The gas transfer rate is dependent on the p_{CO}, which decreases over time. Therefore the maximum transfer rate of CO decreases when CO is consumed. Thus as long as the WGS activity increase, the system is not gas transfer limited, only when it starts decreasing. Initiation of transfer rate limitation results in a decreasing rate of the WGS. By this theory, the point where gas transfer rate limitation starts can be found by looking for the maximum of the slope of the pressure curve (Figure 9).

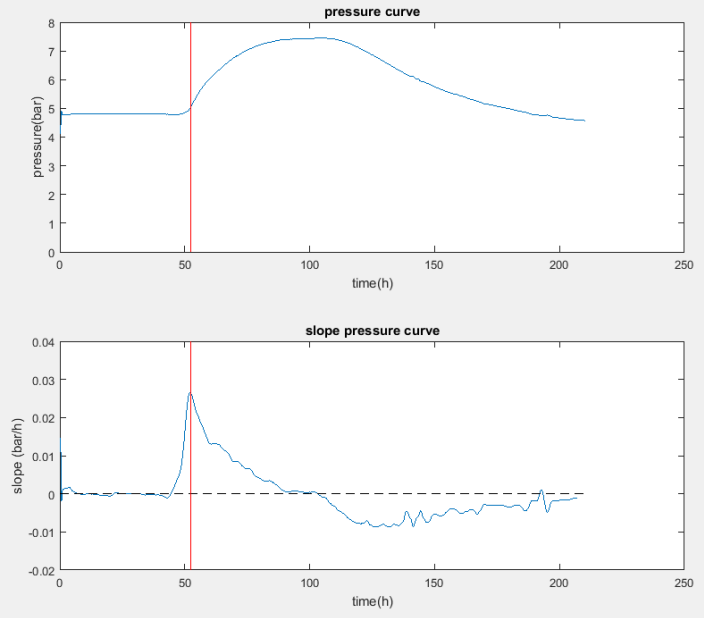

Figure 9. Pressure curve 4A and the corresponding slope. The slope was found by linear regression tough pressure points obtained over 10 minutes. The red line indicates the moment when gas transfer rate limitation starts.

As can be seen in Figure 9, gas transfer rate limitation starts just a few hours after lag the phase ends. Therefore the model will only look into rates after this point. Since during gas transfer rate limitation the CO_L is much lower than its maximum solubility at the given pressure, the contribution CO_L in the CO transfer rate can be neglected (equation 4). This allows for simplification to equation 5.

$$r_{WGS} = k_{COl} * A_L(p_{CO} * m_{CO} - CO_L) \qquad \textit{Equation 4}$$

$$r_{WGS} = k_{COl} * A_L * m_{CO} * p_{CO} = K_{CO} * p_{CO} \qquad \textit{Equation 5}$$

k_{col} CO gas liquid transfer coefficient (m s^{-1}), m_{CO} partition coefficient of CO in water (mol L^{-1} bar^{-1}), CO_L concentration of CO in liquid phase (mol L^{-1}), K_{CO} transfer constant, results from combination of k_{COl}, A_L and m_{CO} (mol s^{-1} bar^{-1})

The yields of CO_2 and H_2 on CO are found to be 0.88±0.04 and 0.77±0.06 mol/mol in the WGS metabolism (appendix page 28). Therefore, it can be assumed that each mol of CO is converted to 1.65±0.04 mol of gas. If it is assumed that when gas transfer limitation starts, the WL pathway has not been active yet, due to the high CO_L before this point. The p_{CO} can be calculated at the point where gas limitation starts using equations 6 to 8.

$$p_{total}^{GL} - \overline{p_{lag}^{total}} = \Delta p_{WGS}^{GL} \qquad \textit{Equation 6}$$

$$\frac{-\Delta p_{WG}^{GL}}{Y_{H2\,CO} + Y_{CO2\,CO}} = \Delta p_{CO}^{GL} \qquad \textit{Equation 7}$$

$$p_{CO}^{GL} = p_{CO}^{t=0} + \Delta p_{CO}^{GL} \qquad \textit{Equation 8}$$

p_{total}^{GL} total pressure when gas transfer limitation starts (bar), $\overline{p_{lag}^{total}}$ average total pressure during lag phase (bar), Δp_{WGS}^{GL} pressure difference due to WGS activity when gas transfer limitation stats (bar), p_{CO}^{GL} CO partial pressure at the start of gas transfer limitation(bar)

With the p_{CO}^{GL} known, the r_{WGS} at the point of gas limitation can be calculated with a estimated value for K_{CO}. If it is assumed that the WL pathway is not active for the first 5 hours after gas limitation, a p_{CO} curve can be produced for the first 5 hours after gas limitation by solving a CO balance over the gas phase (equation 9). This results in a function giving p_{CO} over time for an estimated K_{CO} value (equation 11).

$$\frac{V_G}{R * T} * \frac{d\,p_{co}}{dt} = -K_{CO} * p_{CO} \qquad \textit{Equation 9}$$

$$-\frac{V_G}{R * T} \int_{p_{CO}^{GL}}^{p_{CO}} \frac{1}{p_{co}} * d\,p_{co} = K_{CO} * \int_0^t dt \qquad \textit{Equation 10}$$

$$p_{CO}(t) = p_{CO}^{GL} * \exp\left(-\frac{R * T}{V_G} * K_{CO} * t\right) \qquad \textit{Equation 11}$$

V_G gas volume (m^3), R gas constant (bar m^3 mol^{-1} K^{-1}), T temperature (K).

With the $p_{CO}(t)$ known, the resuling $p_{H2}(t)$ and $p_{CO2}(t)$ can be found by multiplying the consumed p_{CO} with the yield of H_2 or CO_2 in the WGS pathway (equation 12 and 13)

$$p_{H2}^{WGS}(t) = Y_{\frac{H2}{CO}}^{\mathrm{WGS}} * \left(\mathrm{p}_{\mathrm{CO}}^{i} - p_{CO}(t)\right) \qquad \textit{Equation 12}$$

$$p_{CO2}^{WGS}(t) = Y_{\frac{CO2}{CO}}^{WGS} * \left(\mathrm{p}_{\mathrm{CO}}^{i} - p_{CO}(t)\right) \qquad \textit{Equation 13}$$

$$p_{total}^{WGS}(t) = p_{CO}(t) + p_{H2}^{WGS}(t) + p_{CO2}^{WGS}(t) + p_{N2}^{i} + p_{H2O} \qquad \textit{Equation 14}$$

p_{H2}^{WGS} partial H_2 pressure due to WGS activity (bar), $Y_{\frac{H2}{CO}}^{WGS}$ yield of H_2 on CO in the WGS pathway (mol_{H2}/mol_{CO}), p_{CO}^{i} initial CO partial pressure (bar), p_{CO2}^{WGS} Partial CO_2 pressure due to WGS activity (bar), $Y_{\frac{CO2}{CO}}^{WGS}$ yield of CO_2 on CO in the WGS pathway (mol_{H2}/mol_{CO}), p_{total}^{WGS} total pressure due to WGS activity (bar), p_{N2}^{i} initial N_2 pressure, p_{H2O} water vapour pressure (bar).

For each p_{CO} value a corresponding p_{total} can be found with equation 14. For t, a vector containing time values, equal to time values corresponding with the observed pressure points from the Parr system is chosen. This way for each pressure measurement, a corresponding simulated p_{CO} and thus p_{total}, is produced. The difference between the measured and simulated values is dependent on the K_{CO} value, that was estimated earlier. If the K_{CO} is too high, the simulated pressure curve will be too steep while a too low value would result in a simulated pressure curve with a lower WGS rate. The sum of squares between the measured and simulated values is produced. Comparing the sum of squares for a range of K_{CO} values shows a minimum K_{CO} value when the simulation and observed data fit best.

Now that the K_{CO} has been estimated, it can be used to simulate the total pressure curve over the entire length of the experiment, after gas transfer limitation starts, using equations 11 to 14. This simulation only takes gas production by the WGS pathway into account. WL pathway activity is not incorporated in the simulated pressure curve. when the simulated pressure curve is compared to the observed pressure curve, it can be seen that there is a large deviation, that increases over time (Figure 10).

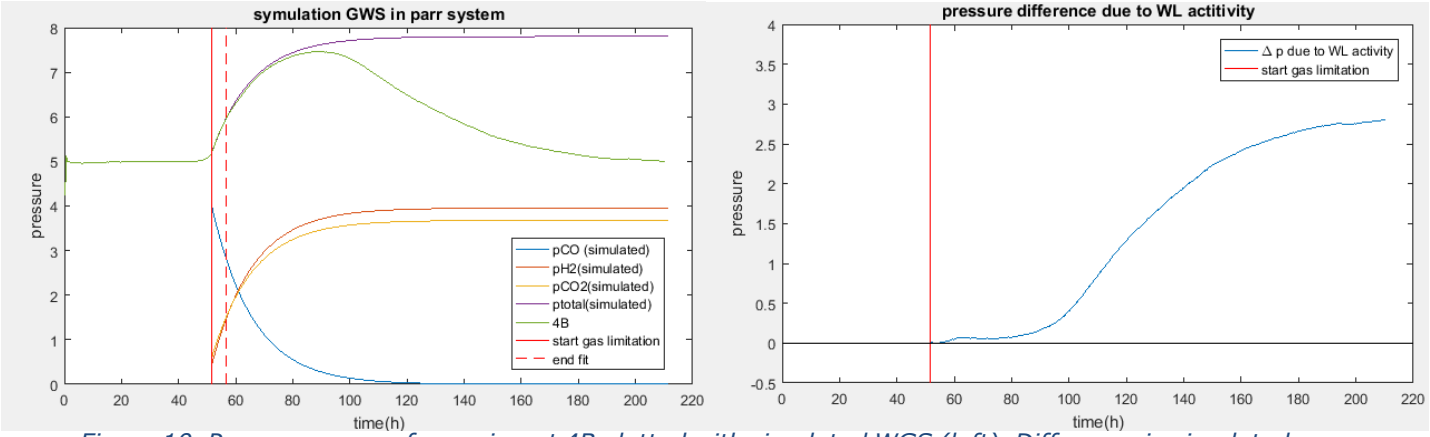

Figure 10. Pressure curve of experiment 4B plotted with simulated WGS (left). Difference in simulated and observed pressure, due to WL pathway activity (right).

In theory, the pressure difference is due to gas consumption by the WL pathway. The slope of this pressure difference gives the activity of the WL pathway. The activity of the WGS pathway is known to be equal to rate of the CO transfer rate (equation5). In Figure 11the rates of both pathway are shown for experiment 4B.

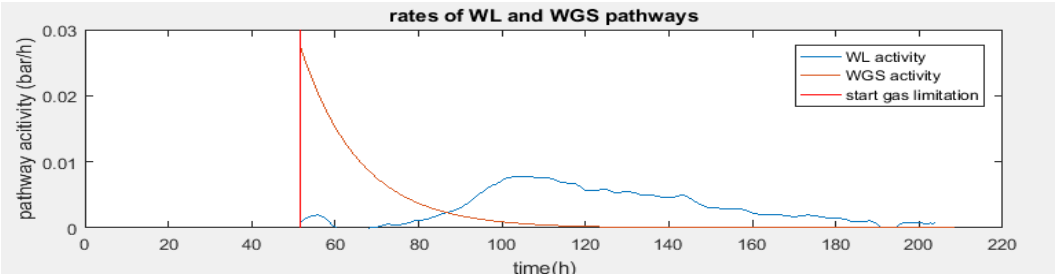

Figure 11. Rates of both WGS and WL pathways

The difference in pressure due to WL activity is combined with the stoichiometry of acetate production in the WL pathway. This is used to predict the H_2 and CO_2 pressures and acetate content over time. In the WL pathway 4 H_2 and 2 CO_2 are required to form 1 acetate (23). However, since CO_2 is partly dissolved, the consumption of 2 mol of CO_2 does not equal the consumption of 2 mol of gaseous substrate. This has to be incorporated in the model. For this Henry's law is assumed (equation 15). At a constant pH of 7 and temperature 70°C a Henry coefficient of 67.0 is used. However, according to the carbonate balance, the pH will decrease if less CO_2 dissolves, decreasing the accuracy of this calculation. Multiplying Henry's law with the gas and liquid volumes gives equation 16.

Equation 15

$$[CO_2]_L = \frac{p_{CO2}}{Kh_{CO2}}$$

Equation 16

$$n_{CO2}^{total} = p_{CO2} * \frac{V_G}{V_M} + \frac{p_{CO2}}{Kh_{CO2}} * V_L$$

$[CO_2]_L$ concentration of CO_2 in liquid phase (mol L^{-1}), n_{CO2}^{total} total mol of CO_2 present in the reactor (mol), V_M molar gas volume (m^3 mol^{-1}), Kh_{CO2} Henry coefficient of CO_2 in water (mol L^{-1} bar^{-1}).

From this equation it can be found that when 1.0 mol of CO_2 is consumed, 0.57 mol of CO_2 is taken from the gas phase. This means that for each 4 mol of H_2 consumed in the WL pathway, 1.14 mol of CO_2 from the gas phase and 0.86 mol CO_2 from the liquid phase will also be consumed. thus $\frac{4}{5.14}$ (78%) of the gas consumed by WL activity is due to H_2 consumption. The remaining 22% is due to CO_2 consumption.

Combining the amount and composition of the gas consumed by the WL pathway with the simulated gas composition due to gas production by the WGS gives the gas composition over time. For this the values for $p_{H2}^{WGS}(t)$ and $p_{H2}^{WGS}(t)$ previously produced by the WGS simulation, can be corrected for the gas consumption by the WL pathway (equation 17 and 18). Adding the yield of acetate on H_2 also gives the amount of acetate produced over time (equation 19).

$$p_{H2}(t) = p_{H2}^{WGS}(t) - \Delta p_{total}^{WL}(t) * f_{H2} \qquad \textit{Equation 17}$$

$$p_{CO2}(t) = p_{CO2}^{WGS}(t) - \Delta p_{total}^{WL}(t) * f_{CO2} \qquad \textit{Equation 18}$$

$$n_{ace}^{WL}(t) = \Delta p_{total}^{WL}(t) * f_{H2} * \frac{V_G}{R * T} * Y_{\frac{ace}{H2}}^{WL} \qquad \textit{Equation 19}$$

Δp_{total}^{WL} pressure difference between simulated WGS pressure and measured pressure (bar), p_{H2} H_2 partial pressure (bar), f_{H2} fraction of H_2 in gas consumption due to WL pathway, p_{CO2} CO_2 partial pressure (bar), f_{CO2} fraction of CO_2 in gas consumption due to WL pathway, p_{CO2} CO_2 partial pressure (bar).

4 Model results

4.1.1 Modelling data at initial CO pressure of 4 bar

Shown below in Figure 12 are simulated and observed pressure curves of experiment 4B. In Table 3Error! Reference source not found. the simulated and measured results are compared. p_{CO} at peak p_{total} were predicted to be between 0.09 and 0.29 bar. This is in line with what was found in experiments 4D and 4E. Furthermore, total amount of acetate is accurately predicted by the simulation. The final p_{H2} is consistently predicted to be lower than was actually observed. Combining this with a consistently overestimated final p_{CO2} gives reason to believe that the ratio between H_2 and CO_2 consumed was not accurately described in the model. This could be due to the error in the ratio between dissolved and gaseous CO_2. If, in reality the solubility of CO_2 was lower than assumed by the henry coefficient at 70°C at a pH of 7, more of the CO_2 would be present in the gas phase. This would increase the f_{CO2} and decrease the f_{H2} term in equation 17 and 18. The pH has an influence on the solubility of CO_2. In the Parr system, pH could not be measured. Errors induced by wrong pH estimation are thus to be expected. A second possibility for an error in distribution of gaseous and solubilised CO_2 could be due to CO_2 not being in its equilibrium distribution. Equation 16 assumes CO_2 in gas and liquid phase are in equilibrium, if this is not the case and error in f_{CO2} and f_{H2} would be induced. In both cases, since less H_2 would be consumed than the model predicts. This would also result less acetate being produced, resulting in an increase of the error in the prediction of final acetate content.

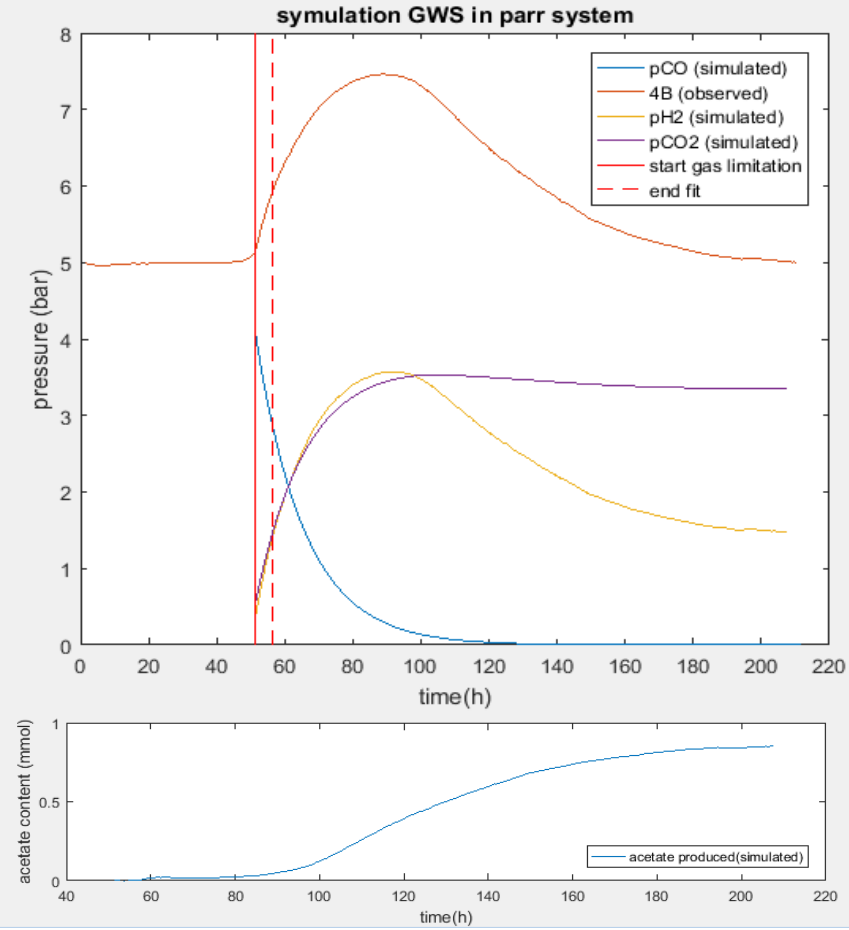

Figure 12. Modelled partial and total pressures curves from the observed pressure of experiment 4 (top). Acetate produced over time, as predicted by model (bottom)

Table 3. . Comparison of simulated and observed final composition of experiments 4A-C.

	4A			**4B**			**4C**		
	Sim	*observed*	*error(%)*	*Sim*	*observed*	*error(%)*	*Sim*	*observed*	*error(%)*
acetate (mmol)	0.89	0.89	0.0	0.85	0.87	-2.3	0.75	0.85	-11
pH2 (bar)	1.24	1.71	-27	1.47	1.88	-21	1.5	1.89	-20
pCO2 (bar)	3.2	3.05	4.9	3.34	3.32	0.6	3.15	3.01	4.7
Kco	8.89E-06			8.54E-06			8.97E-06		

4.1.2 Modelling data at initial CO pressure of 2.7 bar

When the model was applied on the pressure curves of experiment 2.7A and 2.7C, no accurate value for K_{CO} could be found. This set of experiments was set up with a high initial biomass concentration and a lower initial p_{CO}. Therefore the WL pathway could have started to activate during the K_{CO} fitting period. In theory the K_{CO} value should not be dependent on biomass concentration or p_{CO}, only reactor geometry and settings. Therefore the average K_{CO} value found from the data of experiment 4A-C was applied to simulate pressure and acetate content during experiment 2.7A and 2.7C. A comparison of the simulated and observed results can be found in Table 4**.**

Table 4. Comparison of simulated and observed final composition of experiments 2.7A and 2.7C. 2.7B did not show activity. For K_{CO} the average value from experiments 4A-C is used.

	2.7A			**2.7C**		
	Sim	*observed*	*error(%)*	*Sim*	*observed*	*error(%)*
acetate (mmol)	0.36	0.41	-12	0.08	0.13	-38
pH2 (bar)	1.23	1.19	3.4	1.54	1.29	19
pCO2 (bar)	2.00	1.95	2.6	1.65	1.45	13
Kco	0.41	0.43	-4.7	0.92	1.28	-28

Judging for the error between the model and observed values in 2.7A in Table 4, the assumption that K_{CO} is constant though experiments is valid for this experiment. In experiment 2.7C the errors are larger. Since both the simulated p_{H2} and p_{CO2} are too high and the final p_{CO} too low, the rate of the WGS pathway must have been overestimated. The actual K_{CO} value during this experiment is thus expected to be lower than the one applied.

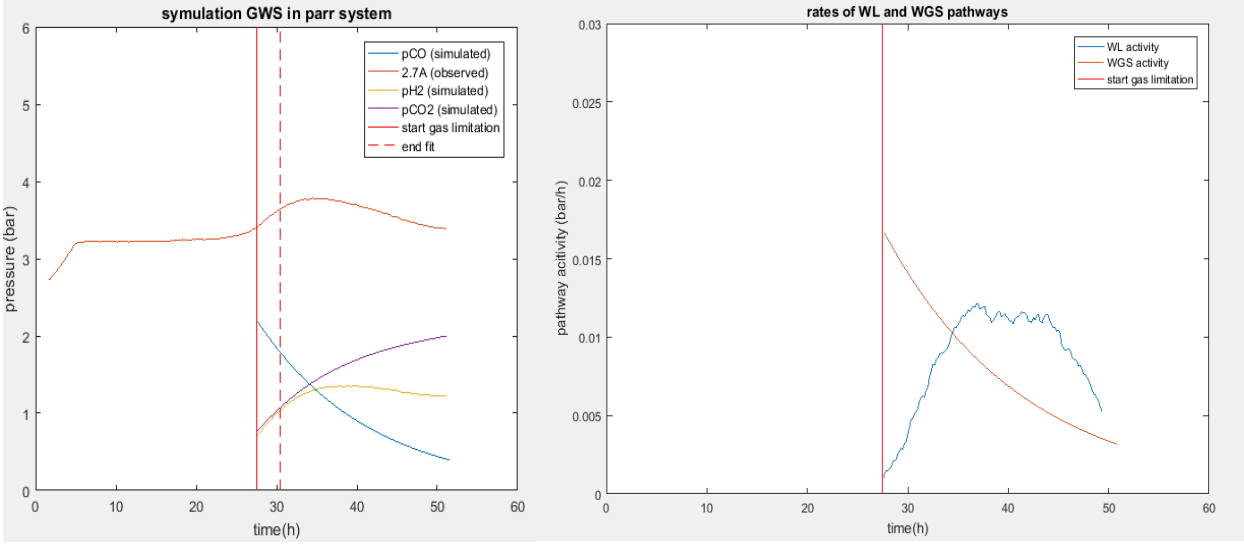

Figure 13. Model outputs for experiments 2.7A. Partial pressures and acetate content shown left. Pathway activity on the right.

The pathway activities shown by the model in experiment 2.7A give an unexpected result. since the model predicted the final composition of this experiment rather accurately, it has to looked into. Judging from the total pressure levelling out towards the end of the experiment (Figure 13), it would be expected that the activity of the organism has stopped. However, the activities calculated by the model show that there is still conversions taking place. Acetate is still accumulating. The gas production and consumption rates of both pathways cancel each other out, resulting in a stable pressure.
The model suggest that during the pressure increasing phase, the CO_L was inhibiting the activity of the WL pathway. Due to the consumption of CO the p_{CO} decreased en the biomass concentration increased. Both contribute to a decrease in the CO_L, decreasing inhibition of the WL pathway. This results in a rapid increase in the rate of the WL pathway. The activity of the WL pathway's resulted a decrease in p_{H2}. Due to the decrease in p_{H2}, the rate of the WL pathway decreased again, until it balanced out with the rate of the WGS pathway.Continiuation of this experiment would have been very valueable, however since it was assumed the activity had stopped, the experiments was stopped aswell.
It can be said with certainty that a same phenomena did not occur in experiments 4A-C since the final p_{CO} values were close to 0. This is due to the fact that WGS pathway was active for 150h in expriments 4A-C compared to 50h in 2.7A.

The model could not be verified for experiment 4F-H since no final liquid of gas data is available.

4.2 WGS and WL Pathway activities

When the activities of the pathway activities of experiments 4A-C (low initial C_x) are compared to those of experiments 4F-H (high initial (C_x), a clear difference is observed. In Figure 14 a slight increase in activity of the WL pathway directly after gas transfer limitation starts can be found in experiment 4B. This is probably due to inaccuracy of the model and is thus ignored. In this experiment WL pathway only starts to show considerable activity after 100h. During experiment 4F the WL pathway activates almost directly after the gas transfer limitation starts. Since the model was not produced to handle such situations the results are uncertain. It does however support the theory mentioned above that the higher biomass concentration in experiments 4F-G decreases the CO_L and thus activates the WL pathway sooner.

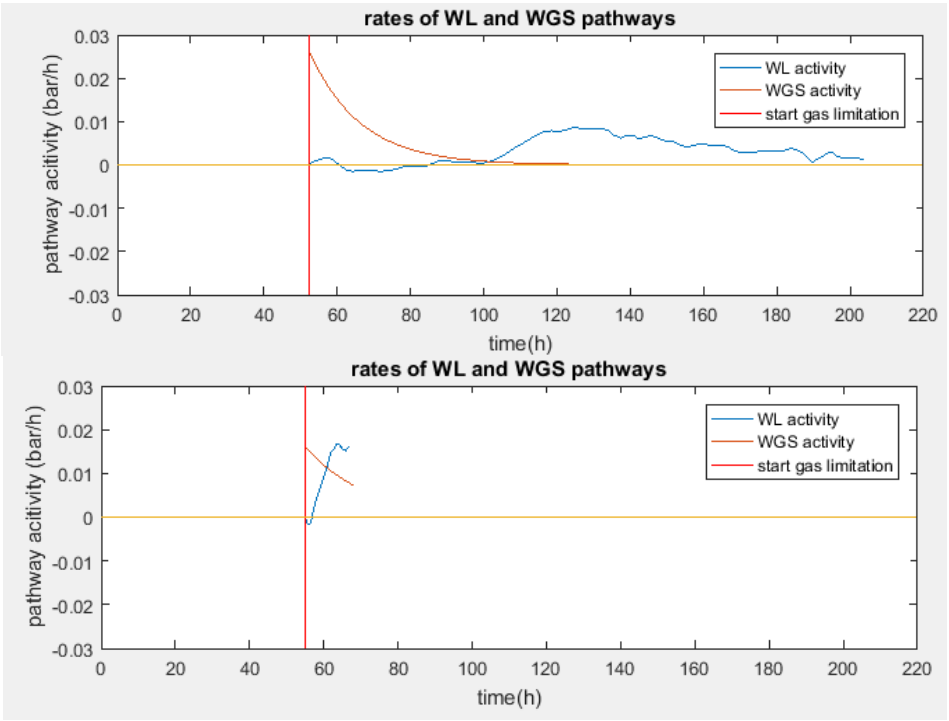

Figure 14. WGS and WL pathway activities during fermentation in experiment 4A (top) and 4F (bottom).

4.3 Model limitations

As mentioned above, the model is designed to handle situation in which the WL pathway is not active during the first few hours after the gas transfer limitation starts. This is due to the model assuming all the change in pressure is due to WGS during this period. With more data, a better estimation of K_{CO} could be made, making it possible to model situation in which the WL is active during the first hours. This has already been shown to have some success in the modelling of experiments 2.7A and 2.7C. A second limitation in the way the model is set up, is that it requires a pressure curve input to predict partial pressure and acetate accumulation. For the WGS pathway activity the pressure curve can be replaced by finding an average K_{CO} value. This would than generalise the rate of the WGS pathway after gas limitation starts. The rate of the WL pathway is calculated by the difference between the total pressure expected when only the WGS pathway is active and the measured pressure. Thus the WL pathway cannot be simulated without a pressure curve. Since the rate of the WL pathway is dependent on the CO_L concentration, which cannot be measured over time, a different approach for modelling the activity is not an option at this point. A second unknown would be the final pressure. Theoretically the WL pathway should be able to continue when enough H_2 is present. However, for *C. hydrogenoformans* it seems to stop under a certain set of conditions. From the set of experiments conducted in this research, no relation between final p_{H2} and experiment setup was found.

5 Conclusion

In this research it has been shown that *C. hydrogenoformans* can produce acetate from CO at 70°C in a two-step process. First CO is converted into H_2 and CO_2 through the WGS pathway. Production of acetate through the WL pathway is more complex. It is influenced by H_2 pressure and CO concentration in the liquid phase. If the concentration of CO in the liquid phase is too high, it inhibits the activity of the WL pathway. This research was not able to produce a CO concentration at which the WL pathway becomes active. It was found to be low enough, that CO_L concentrations fully inhibiting WL activity did not visibly affect the gas transfer rate of CO. WL pathway activity stopped while all substrates were still present, indicating the requirement of an elevated H_2 pressure to drive this pathway.

6 Effect of biological conditions on RU/c catalyst activity

Now that the a better understanding of the acetate production with *C. hydrogenoformans* has been gained, the in situ hydrogenation to ethanol on Ru/C can be further looked into. Three unknowns in combining the biological and chemical conversion are investigated in this research. First the hydrogenation of CO is looked into. Secondly, the viability of *C. hydrogenoformans* in presence of the Ru/C is tested. Finally the viability of Ru/C under biological conditions and. A third possible problem for combination of the conversions is hydrogenation of CO. both are assessed in this section.

6.1 CO hydrogenation

If the Ru/C hydrogenates CO to methane, it will compete for CO with the organism. This could result in a decrease in acetate production due to formation of methane. If this hydrogenation occurs, CO would already be consumed during the lag phase of *C. hydrogenoformans*. This would decrease the overall yield of acetate on CO. The toxicity of methane of *C. hydrogenoformans* has also not been studied. If Ru/C hydrogenates CO to formate, but not methane, the formate could theoretically be consumed by the organism in the WL pathway. No data on this is available. To test if Methane is produced, the parr system is setup with 200mg 5%wt Ru/C in MQ, a p_{CO} of 4 bar and a p_{H2} of 16 bar (room temperature). After 3 days at 70°C, no methane or soluble products were detected.

6.2 Cell viability

Since, too our knowledge, this is the first time cell are cultivated in the presence of metallic ruthenium, the viability of the cells is yet unknown. To test this Ru/C catalyst was added to biological medium containing *C. hydrogenoformans*. Biological activity was monitored by measuring the H_2 production and CO consumption.

In all four cultures containing Ru/C, all CO was consumed within 5 days of inoculation. When compare to a duplicate blanc, not containing Ru/C, no significant difference in final H_2 content was observed. Cell are thus active in the presence of Ru/C.

The Ru/C was recovered through filtration and dried. Hydrogenation activity was tested over 72h in 10%wt acetic acid with 200 mg 5% Ru/C at a hydrogen pressure of 58.5 bar. Final ethanol content did not exceed 0.05 mmol for all samples. This is considerably lower than described by previous research (20). The Ru/C catalyst is thus deactivated under biological conditions. One theory on how the biological conditions deactivate the catalyst is through formation of a biofilm. If a biofilm were to grown onto the catalyst particles, this could plug the pores in the carbon support. Without the pores the majority the active surface area would be blocked, deactivating the catalyst. To test this theory, samples of catalyst, before hydrogenation, were freeze dried and analysed by SEM.

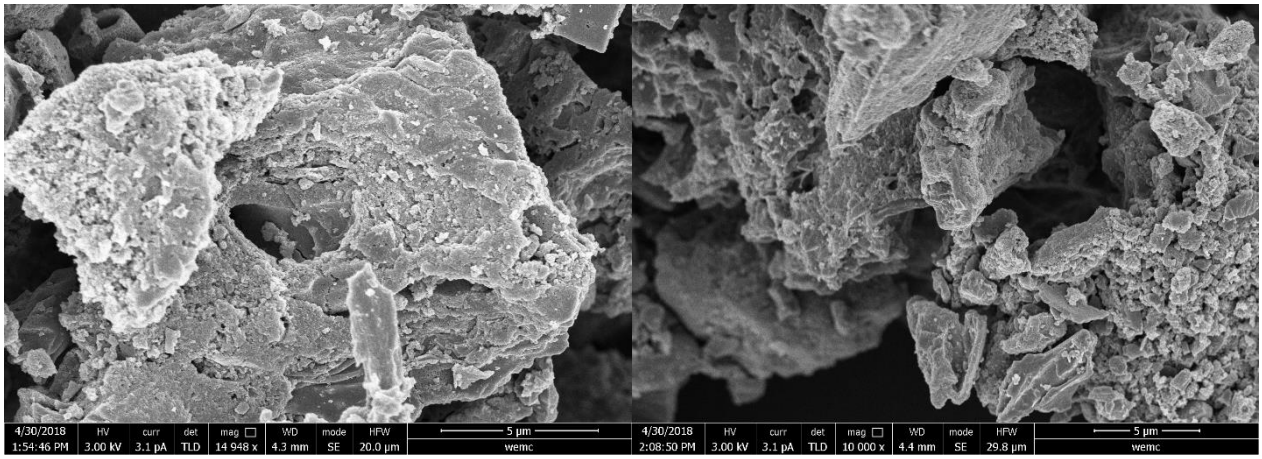

Figure 15. SEM pictures of 5%wt. Ru/C incubated in biological medium at 70°C for 5 days with C. hydrogenoformans (left) and under sterile conditions (right).

It has been documented that cells are rod shaped and between 1.3 and 2.4µm long (17). These should be clearly visible in the SEM images, yet they are not observed (Figure 15). Deactivation of the catalyst was thus not due to blockage of the pores. Since no physical deactivation of the catalyst was observed, chemical deactivation by medium components (poisoning) was looked into. To identify which compounds present in the medium affect catalyst activity, a new set of experiments was conducted.

6.4 Catalyst stability in CP-medium

To identify which compounds in the biological medium have interactions with the catalyst, reducing its activity, the medium was broken down in several components. These where added to the catalyst in the same concentration than they are found in the growth medium. The medium was broken up into a salt fraction, Ca^{2+}/vitamin solution, YE, biomass and sulfide. The hydrogenation activity is tested in the same setup as described above.

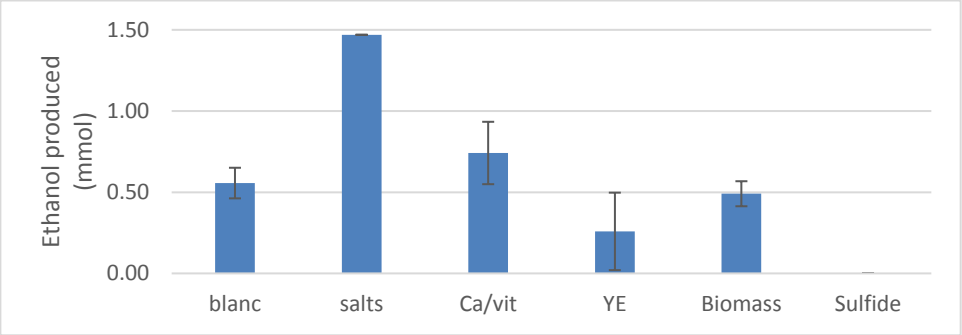

Figure 16. Effect of medium components on ethanol production. Final ethanol content after 72h reaction of acetic acid to ethanol with Ru/C under a hydrogen pressure of 58 bar at 70°C with varying medium components added. All measured in duplicate, except for salts and sulphide due to leakage. Standard deviation given by error bars.

Due to leakage of hydrogen in one of the samples to which salt was added and one where sulphide was added, these experiments have not been executed in duplicate. Unfortunately these also show some of the most interesting results. The sample to which salts were added show a final ethanol content that is more than double the blanc measurement. Since it was shown that the addition of salts did not affect the activity of Ru/c catalysed lactic acid hydrogenation (33) it is unlikely that these salts function as a promotor and this result is considered to be an outlier.. Furthermore, in literature. In this research it was also observed that the presence of contaminating proteins reduced the activity of Ru/C hydrogenation. Therefore it was expected that adding YE or biomass would reduce catalyst activity. However no significant difference in final ethanol content was observed ($p>0.05$). In the above mention research a trickle bed reactor was used, loaded with 5% wt. Ru/C catalyst. To this system lactic acid, containing varying fermentation contaminations, was added. Once bovine serum was added, as a model impurity, the lactic acid conversion decreased from 55% to 35% (33). The data in Figure 16, showing the final ethanol content with YE added, seems to be in line with the results described in the paper. However due to the lack of accuracy in this experiment, this cannot be said with any certainty. Furthermore it was expected that adding biomass and YE would have similar effects, since YE essentially is biomass. From the results it seems that YE has a stronger deactivating effect on the catalyst. However, since the biomass concentration could not be measured with any accuracy, the concentration of biomass in this experiment is unknown. It could have the same deactivating effect as YE, but due to a lower concentration of biomass being applied, compared to YE, a higher final ethanol content is achieved in these samples.

When sulfde was added no ethanol was produced. this was expected since deactivation of ruthenium based catalyst by sulfur compounds has been observed before on other supports (19, 21, 27).

6.5 Medium optimisation

In the previous experiment it was found that catalyst deactivation mainly occurs by sulfide and to a lesser extend YE. It was already found that cells can be active without YE being added (Figure 4). Some YE will be present due to the YE in the inoculum. However, it is expected that such low concentrations will not have a large impact on the hydrogenation activity.

Several attempts have been made to grow *C. hydrogenoformans* without sulfide present. These were not successful. Sulfide is added as a reducing agent to remove the last traces of O_2 present in the medium. Since *C. hydrogenoformans* is a strictly anaerobic bacterium (24) , even trace amounts of oxygen can inhibit all activity. It was attempted to remove more oxygen from the medium by flushing the headspace with N_2/CO_2 daily for 5 days in a row, before cells were added. This did not result in growing culture. The

resazurin present in the medium showed a light pink colour, indicating O_2 presence. Active cultures were obtained when an inoculum volume of 4.0 mL, instead of the normal 0.5 mL, was used. In this case the sulfide present in the inoculum was enough the reduce the medium (data not shown). The concentration of sulfide required was thus lowered, but removing sulfide completely was not possible. The exact amount of sulfide applied during this large inoculation is unknown, since sulfide is consumed when it is oxidised or when is serves as a sulfur source for the bacterium.

There are other reducing agent that can replace the role of sulfide, such as cysteine. However, since these compounds share their strong reducing capabilities with sulfide, catalyst deactivation in their presence is expected (21).

7 Conclusion

Ru/C did not hydrogenate CO at a H_2 pressure of 16 bar and is thus less likely to compete for H_2 with *C. hydrogenoformans*. Full deactivation of Ru/C was observed when it was introduced to biological medium. Sulfide is the strongest deactivator. Yeast extract also showed to have some deactivating function. In combined cultivation, biofilm formation was not observed.

8 summary

In this work, individual elements of a combined biological and chemical syngas conversion, utilising *C. hydrogenoformans* and Ru/C have been studied. It was found that *C. hydrogenoformans* is able to produce acetate from CO in a two-step process in which CO is first converted to H_2 and CO_2 in the water gas shift pathway, followed by acetate production from H_2 and CO_2 though the Wood-Ljungdahl pathway. Inhibition of CO on the Wood-Ljungdahl pathway was observed, with inhibition being stronger at a lower biomass concentration and higher CO pressure. Attempts to activate the Wood-Ljungdahl pathway without prior water gas shift activity were unsuccessful.

The Ru/C catalyst was shown not to hydrogenate CO under a H_2 pressure of 16 bar at the biological temperature of 70°C. Deactivation of the catalyst was observed when incubated with *C. hydrogenoformans* for 5 days. No sign of sterical deactivation were observed through SEM imaging. The Ru/C was shown to fully deactivate due to poisoning by sulfide, that is essential for biological activity. The only other biological medium component that showed signs of inhibition was yeast extract. However, results were inconclusive.

9 recommendations

This research resulted in a good basic understanding of the acetate metabolism in *C. hydrogenoformans*, though some aspects could be worth studying further. In this work, some attempts were made to activate the WL pathway, without the presence of CO. These attempts were unsuccessful. The biomass concentration in these attempts was much lower than the concentration during the WL-phase in the higher pressure CO fermentation experiments. A possible theory is that the WL activity is only a background activity, not a fully functional energy metabolism. Due to the high biomass concentration, still a high overall WL rate is observed in high pressure CO fermentation experiments. Due to the much lower biomass concentration in the CO spike experiment, a very low WL activity was observed.

the failure activate the WL pathway without CO present could also be due to the protocol used to setup the reactors with only H_2 and CO_2. This is a long and delicate process with many opportunities for mistakes. Most of these mistakes will only become apparent when the reactors are opened. Improving the current reactor system to a system that is easier to setup, would increase the success rate of experiment. A second interesting parameter to study would be the stirring rate in the Parr system. In this research a low stirring rate was chosen (200rpm). Increasing the stirring rata would increase the K_{CO}, resulting in a higher CO_L. This should both increase the rate of the WGS pathway and decrease the WL pathway activity, if the abovementioned theory is correct.

To study the effect of CO inhibition and role of H_2 pressure on the WL, a continuous reactor would be required. Combined with live pH monitoring, this system would allow for more accurate predictions of dissolved CO_2 and CO concentration, inhibition due to low pH and H_2 reduction potential. Operating in continuous mode would also show if *C. hydrogenoformans* can survive utilising the WL pathway for energy generation. Furthermore, by controlling the composition of gas inflow in such a continuous system, the extend of CO inhibition on the WL could be identified. However, since continuous system that can operate under high pressure are scares and expensive, the likelihood of the availability of such system is low. When the Ru/C stability under biological condition was tested, is was shown that sulfide fully deactivated the catalyst. Yet *C. hydrogenoformans* was not able to be active without sulfide present. Since sulfide is added as a reducing agent to remove final traces of oxygen, an alternative has to be found. It was found that oxygen contaminated cultures could be revitalised by adding additional sulfide. Thus in presence of oxygen, not all cells are killed. Therefore, in theory, a co-culture of *C. hydrogenoformans* and a CO tolerant facultative aerobic organism could result in activity of *C. hydrogenoformans*. In such a system the facultative organism would be given a substrate that it could both ferment and oxidise with O_2. This would activate the facultative organism, removing all O_2 through its aerobic metabolism. At this point *C. hydrogenoformans* could become active. Since *C. hydrogenoformans* has been shown to grow on a very limited range of substrates (17), it would not compete with the other organism.

10 appendix

10.1Improving Parr system setup

In previous work from the department of Biobased Chemistry and Technology, acetate concentration up to 68 mM have been achieved, using *C. hydrogenoformans* (18). This was done by increasing the initial p_{CO}. Since this is not feasable in shake flasks, in an autoclave reactor (Parr system) was used. When the Parr system was used in previous work, data was not reproducible. Large variation in lag phase and final CO content were found (18). During early trials it was found that flushing the reactor vessels with N_2/CO_2 (4:1) before adding CO helped to obtain more stable results (data not shown). The CO_2 added during this procedure balances with the $NaHCO_2$ in the liquid at a pH around 7. A detailed description of the reactor setup procedure can be found in the appendix. A second factor that could influence the reproducibility of the results is the temperature overshoot. Due to the setup of the Parr system, when heating the reactors to the desired temperature of 70°C, an overshoot exceeding temperatures of 80°C was observed. Growth of *C. hydrogenoformans* stops at a 78°C (17). Temperatures exceeding this limit could result in cell death. Since the peak temperature and the duration of the overshoot varied ammong experiments, the active biomass concentration at the start of fermentation could have varied as well. To prevent this a 4h temperature ramp was programmed, instead of setting the system to heat to 70°C directly. In this improved setup *C. hydrogenoformans* was grown under an initial p_{CO} ranging from 1.2 to 4 bar.

10.2 WL activity at 1.2 bar CO

The experiment previously described on page 10 has been redone. As can be seen in Figure 17, no pressure decreasing phase is observed with an initial CO partial pressure of 1 bar, if incubation time is increased.

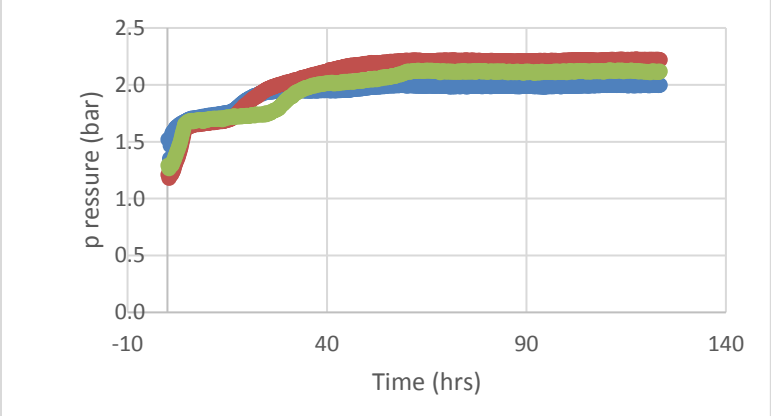

Figure 17. Repetition of experiment 1.2A-C. Due to difficulties reproducing initial CO pressure an initial CO pressure of 1.0 bar was applied.

10.3 Yield of H_2 and CO_2 in WGS

To find the yield of H_2 and co_2 in the WGS pathway an experiment was conducted in shake flasks. In this experiment 3 117mL shake flasks were filled with 52 mL medium and inoculated with 0.5 mL active culture. The experiment has been stopped before all CO is consumed to reduce WL pathway activity.

Table 5 shows results of the duplicate gas measurements at the end of incubation and headspace composition during inoculation. Final yields of H_2 and CO_2 were found to be 0.88±0.04 and 0.77±0.06 mol/mol respectively. CO_2 yield is lower than H_2 yield due to the solubility of CO_2. Solubilised CO_2 was not added to the calculation. To do this, pH measurements under the final CO_2 pressure are required, which are not possible.

Table 5. Gas composition before and after fermentation. Tested in triplicate, each flask measured in duplicate

	CO t=0 *(mmol)*	*CO2 t=0* *(mmol)*	*H2 t=0* *(mmol)*	*CO final* *(mmol)*	*H2 final* *(mmol)*	*CO2 final* *(mmol)*	$Y_{H2/CO}$ *(mol/mol)*	$Y_{CO2/CO}$ *(mol/mol)*
A	3.24	2.09	0.00	1.37	1.65	3.55	0.88	0.78
A	3.24	2.09	0.00	1.39	1.69	3.61	0.92	0.83
B	3.19	2.09	0.00	1.45	1.49	3.37	0.86	0.74
B	3.19	2.09	0.00	1.52	1.57	3.48	0.94	0.84
C	3.12	2.09	0.00	1.02	1.78	3.60	0.85	0.72
C	3.12	2.09	0.00	1.01	1.76	3.55	0.84	0.69
						avg	0.88	0.77
						stdev	0.04	0.06

10.4 CO spike experiment

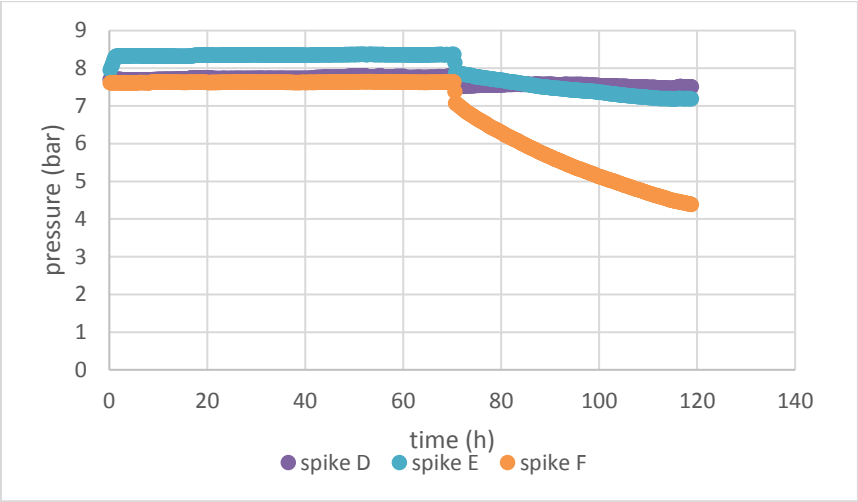

Figure 18. Pressure curves output of the Parr system with C. hydrogenoformans under 1 atm N2/CO2 (4:1), 4.0 bar H_2 and 3.0 bar CO_2. Pressure drop at t=70h indicates opening on the valves

In Figure 18 results from the CO spike experiment are shown. In reactors E and F, leakage in the tubing was detected. This is observed in the pressure curve and verified with leak detection spray. No conversion was measured in any of the reactors. Two out of the five reactors showed pink medium during opening of the reactors. This indicated contamination of oxygen. Since it is difficult to make this observation while shutting down the system it cannot be said if more reactors showed this phenomena. A possibility is that the CO_2 stock is contaminated with oxygen. The H_2 stock was used in other experiments with *C. hydrogenoformans* (data not shown) without deactivation of the culture. Thus the H_2 stock is not the cause of a possible oxygen contamination.

Table 6 shows the final acetate concentration measured after the CO spike experiment. Values were corrected for acetate produced for YE. These values confirm that the WL pathway was not active during this experiment.

Table 6. Final acetate content CO spike experiment

name	*Acetate (mmol)*
Spike B	-0.041
Spike C	-0.025
Spike D	0.073
Spike E	-0.010
Spike F	-0.072

10.5 Effect of high initial H_2 pressure on acetate production

To test investigated if the WL pathway does show activity when exposed to only a high H_2 pressure A set of shake flask experiments was setup. These flasks only held a CO_2 pressure of 0.2 bar to avoid pH shock. Shake flasks were filled as shown in Table 7. In theory the H_2 pressure should be sufficient to activate the WL pathway, since at the applied H_2 pressures WL activity was observed in experiment 4A-C. CO was added to all samples to allow a short WGS phase to energy generation, however to samples C and D only 1 mL was added.

Table 7. Initial partial pressures in high pressure shake flask experiments

	p_{CO2} *(bar)*	p_{H2} *(bar)*	p_{CO} *(bar)*
A	0.2	0.8	0.65
B	0.2	2.4	0.65
C	0.2	0.8	0.03
D	0.2	2.8	0.03

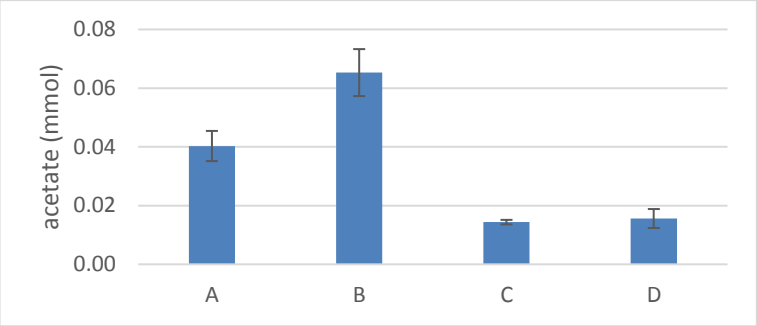

Figure 19. Final acetate content high pressure shake flask experiments, corrected for background acetate by YE conversion. Measured in triplicate, error bars represent standard deviation

After five days of incubation a significantly higher acetate content was found in samples B compared to samples A (p=0.01). This implies that at a higher p_{H2} more acetate is produced. The WL pathway is thus dependent on the p_{H2}. If however the results of samples C and D are compared, no significant difference in final acetate content is found (p=0.29). It would be expected that in samples D a higher final acetate content would be measures, due to the higher p_{H2}. However it did not. In this set of experiments the WL pathway activity observed in 4A-C could not be reproduced.

10.6 Mathematical derivation of WL activity at high C_X

Theoretically, the observed rate of the WL pathway is equal to equation 1, assuming competitive inhibition of CO (34).

$$r_{WL} = q_{WL}^{max} * \frac{[S]}{K_m * \left(1 + \frac{CO_L}{K_i}\right) + [S]} * C_x * V_L \qquad \textit{Equation 20}$$

r_{WL} rate of the WL pathway (mol h^{-1}), q_{WL}^{max} maximum activity of the WL pathway (mol $gram_{biomass}^{-1}$ m^{-3} h^{-1}),$[S]$ substrate conentration (mol L^{-1}), K_m Michalis Menten constant (mol L^{-1}), CO_L CO concentration in the liquid (mol L^{-1}), K_i inhibition constant (mol L^{-1}),C_x biomass concentration (gram L^{-1}) and V_L liquid volume (L).

In experiment 4F-H, the biomass concentration at the start of fermentation was 15 times higher than that in experiment 4D-E. However, since the activity of the WL pathway was close to 0 in 4D-E, even after more than 90% of the CO was consumed, multiplying this low activity with a C_x that is 15 times greater would not result in a large difference in r_{WL}. Since all other parameters except CO_L are set, the CO concentration in the liquid must be lower in experiments 4F-H in order to have a higher r_{WL}. Equation 1 shows that the r_{WL} can be very sensitive towards changes in CO_L, if the K_i is close to the value CO_L.

To find if higher biomass concentrations lead to lower CO_L values, the rate of the WGS pathway has to be looked into. Assuming Monod's kinetics for the activity of the WGS pathway (equation 2) and a the rate of the WGS being equal to the gas transfer rates of CO (equation 3) gives equation 4. From this equation it can be seen that when the biomass concentration is increased, the left hand side of the equation would become larger. To compensate for this the CO_L would have to decrease. This does not have an considerable impact on the gas transfer rate, since the CO_L was already close to 0. It will however have a large impact on the Monod kinetics of the WGS pathway's activity.

$$r_{WGS} = q_{WGS}^{max} * \frac{CO_L}{K_m + CO_L} * V_L * C_x \qquad \textit{Equation 21}$$

$$r_{WGS} = k_{COl} * A_L(p_{CO} * m_{CO} - [CO]_L) \qquad \textit{Equation 22}$$

$$q_{WGS}^{max} * \frac{CO_L}{K_m + CO_L} * V_L * C_x = k_{COl} * A_L\left(p_{CO} * m_{CO} - [CO]_L\right) \qquad \textit{Equation 23}$$

r_{WGS} rate of the WGS pathway (mol h^{-1}), q_{WGS}^{max} maximum activity of the WGS pathway (mol $gram_{biomass}^{-1}$ m^{-3} h^{-1}), k_{COl} transfer rate of CO into liquid (m s^{-1}), A_L gas liquid interface area (m^2), p_{CO} CO partial pressure (bar), m_{CO} partition coefficient CO (mol L^{-1} bar^{-1}).

References

1. Huber GW, Iborra S, Corma A. Synthesis of transportation fuels from biomass: chemistry, catalysts, and engineering. Chemical reviews. 2006;106(9):4044-98.
2. Ragauskas AJ, Williams CK, Davison BH, Britovsek G, Cairney J, Eckert CA, et al. The path forward for biofuels and biomaterials. science. 2006;311(5760):484-9.
3. Fernando S, Adhikari S, Chandrapal C, Murali N. Biorefineries: current status, challenges, and future direction. Energy & Fuels. 2006;20(4):1727-37.
4. Kirubakaran V, Sivaramakrishnan V, Nalini R, Sekar T, Premalatha M, Subramanian P. A review on gasification of biomass. Renewable and Sustainable Energy Reviews. 2009;13(1):179-86.
5. Franco C, Pinto F, Gulyurtlu I, Cabrita I. The study of reactions influencing the biomass steam gasification process☆. Fuel. 2003;82(7):835-42.
6. Yung MM, Jablonski WS, Magrini-Bair KA. Review of catalytic conditioning of biomass-derived syngas. Energy & Fuels. 2009;23(4):1874-87.
7. Couto N, Rouboa A, Silva V, Monteiro E, Bouziane K. Influence of the Biomass Gasification Processes on the Final Composition of Syngas. Energy Procedia. 2013;36:596-606.
8. Kamm B. Production of platform chemicals and synthesis gas from biomass. Angewandte Chemie International Edition. 2007;46(27):5056-8.
9. Bredwell MD, Srivastava P, Worden RM. Reactor design issues for synthesis-gas fermentations. Biotechnology progress. 1999;15(5):834-44.
10. Munasinghe PC, Khanal SK. Biomass-derived syngas fermentation into biofuels: opportunities and challenges. Bioresource technology. 2010;101(13):5013-22.
11. Kundiyana DK, Huhnke RL, Wilkins MR. Syngas fermentation in a 100-L pilot scale fermentor: design and process considerations. Journal of bioscience and bioengineering. 2010;109(5):492-8.
12. Diender M, Stams AJ, Sousa DZ. Production of medium-chain fatty acids and higher alcohols by a synthetic co-culture grown on carbon monoxide or syngas. Biotechnology for biofuels. 2016;9(1):82.
13. Chheda JN, Dumesic JA. An overview of dehydration, aldol-condensation and hydrogenation processes for production of liquid alkanes from biomass-derived carbohydrates. Catalysis Today. 2007;123(1-4):59-70.
14. Hu L, Lin L, Liu S. Chemoselective hydrogenation of biomass-derived 5-hydroxymethylfurfural into the liquid biofuel 2, 5-dimethylfuran. Industrial & Engineering Chemistry Research. 2014;53(24):9969-78.
15. Abubackar HN, Veiga MC, Kennes C. Biological conversion of carbon monoxide: rich syngas or waste gases to bioethanol. Biofuels, Bioproducts and Biorefining. 2011;5(1):93-114.
16. Henstra AM, Sipma J, Rinzema A, Stams AJM. Microbiology of synthesis gas fermentation for biofuel production. Current Opinion in Biotechnology. 2007;18(3):200-6.
17. Svetlichny V, Sokolova T, Gerhardt M, Ringpfeil M, Kostrikina N, Zavarzin G. Carboxydothermus hydrogenoformans gen. nov., sp. nov., a CO-utilizing thermophilic anaerobic bacterium from hydrothermal environments of Kunashir Island. Systematic and Applied Microbiology. 1991;14(3):254-60.
18. Hofman J. The effect of change in CO pressure, H2:CO ratio and overall pressure on the matabolism of extremophiles. BCT thesis. 2017.
19. Wentrcek PW, McCarty JG, Ablow CM, Wise H. Deactivation of alumina-supported nickel and ruthenium catalysts by sulfur compounds. Journal of Catalysis. 1980;61(1):232-41.
20. Theobald S. Influence of H_2 partial pressure on the aceata production by etromophiles and *in situ* conversion to ethanol using hetrogeneous ruthenium catalyst. BCT thesis. 2018.
21. Suzuki T, Iwanami H-i, Yoshinari T. Steam reforming of kerosene on Ru/Al2O3 catalyst to yield hydrogen. International Journal of Hydrogen Energy. 2000;25(2):119-26.
22. Olcay H, Xu Y, Huber GW. Effects of hydrogen and water on the activity and selectivity of acetic acid hydrogenation on ruthenium. Green Chemistry. 2014;16(2):911-24.
23. Bertsch J, Müller V. Bioenergetic constraints for conversion of syngas to biofuels in acetogenic bacteria. Biotechnology for biofuels. 2015;8(1):210.
24. Wu M, Ren Q, Durkin AS, Daugherty SC, Brinkac LM, Dodson RJ, et al. Life in hot carbon monoxide: the complete genome sequence of Carboxydothermus hydrogenoformans Z-2901. PLoS genetics. 2005;1(5):e65.
25. Henstra AM, Stams AJ. Deep conversion of carbon monoxide to hydrogen and formation of acetate by the anaerobic thermophile Carboxydothermus hydrogenoformans. International journal of microbiology. 2011;2011.
26. Olcay H, Xu L, Xu Y, Huber GW. Aqueous-Phase Hydrogenation of Acetic Acid over Transition Metal Catalysts. ChemCatChem. 2010;2(11):1420-4.
27. Bartholomew CH. Mechanisms of catalyst deactivation. Applied Catalysis A: General. 2001;212(1):17-60.
28. Rodriguez JA, Hrbek J. Interaction of sulfur with well-defined metal and oxide surfaces: unraveling the mysteries behind catalyst poisoning and desulfurization. Accounts of Chemical Research. 1999;32(9):719-28.
29. Zhao Y, Cimpoia R, Liu Z, Guiot SR. Kinetics of CO conversion into H 2 by Carboxydothermus hydrogenoformans. Applied microbiology and biotechnology. 2011;91(6):1677.
30. Buckel W, Thauer RK. Energy conservation via electron bifurcating ferredoxin reduction and proton/Na+ translocating ferredoxin oxidation. Biochimica et Biophysica Acta (BBA)-Bioenergetics. 2013;1827(2):94-113.
31. Seravalli J, Kumar M, Ragsdale SW. Rapid Kinetic Studies of Acetyl-CoA Synthesis: Evidence Supporting the Catalytic Intermediacy of a Paramagnetic NiFeC Species in the Autotrophic Wood− Ljungdahl Pathway. Biochemistry. 2002;41(6):1807-19.
32. Wilkins MR, Atiyeh HK. Microbial production of ethanol from carbon monoxide. Current Opinion in Biotechnology. 2011;22(3):326-30.
33. Zhang Z, Jackson JE, Miller DJ. Effect of biogenic fermentation impurities on lactic acid hydrogenation to propylene glycol. Bioresource technology. 2008;99(13):5873-80.
34. King EL, Altman C. A schematic method of deriving the rate laws for enzyme-catalyzed reactions. The Journal of physical chemistry. 1956;60(10):1375-8.